MASTER

Calculation on and measurements with the Eindhoven combustion MHD generator with non-uniformities

van Buuren, M.A.

Award date:
1993

EG/93/680

FACULTEIT DER ELEKTROTECHNIEK

Vakgroep Elektrische Energiesystemen

CALCULATION ON AND MEASUREMENTS WITH THE EINDHOVEN COMBUSTION MHD GENERATOR WITH NON-UNIFORMITIES

M.A. van Buuren

Afst. hoogleraar: Prof.dr. L.H.Th. Rietjens
Afst. begeleiders: Dr.ir. W.F.H. Merck
Dr. A. Veefkind

Eindhoven, augustus 1993

TECHNISCHE UNIVERSITEIT EINDHOVEN

ABSTRACT

The MHD generator efficiency improves if the temperature interval, available for the MHD conversion process, increases. To avoid the temperature limitation, caused by the insufficient level of the electrical conductivity at lower gas temperatures, a plasma flow with non-uniformities is proposed. Hot clots take care of the electrical conduction and interact with the cold surrounding gas.

To study the behaviour and lifetime of the clots in the Eindhoven combustion MHD generator, calculations with 1-Dt and 2-Dt codes on and experiments with the Eindhoven shock tube and MHD channel facility have been carried out.

The experiments show that hot clots can be created by means of an electrical discharge. Experiments and calculations show over the length of the channel a decay of the clot temperature. The calculations don't consider diffusion and thermal conduction and the clot temperature decreases due to clot expansion. The clot height is equal to the electrode height; the channel height. Clot expansion in axial and channel width direction takes place because of presence of a pressure gradient between clot and gas. Magnetic interaction causes clot deceleration and disturbance of the gas flow resulting in clot expansion in the channel width direction. Internal dissipation causes increase of the pressure gradient between clot and gas and less decay of the clot temperature.

Experiments and calculations show a decay of the clot temperature over the length of the channel for the condition of 2.5 T magnetic induction. From the 1-Dt calculations it is shown that the condition of 5 T magnetic induction provides for a stable clot temperature because of high internal dissipation. Calculations show that increase of initial clot size extends the clot lifetime. Therefore a gas flow with few large clots is preferable to a gas flow with many small clots. It is better to increase the clot length than the clot width, increasing the initial clot width causes stronger deformation of the clot due to gas flow disturbance. From the 2-Dt calculations it is shown that increasing the initial clot temperature from 3500 to 4100 K results in an extended clot lifetime.

CONTENTS

1. INTRODUCTION

The efficiency of the open cycle combustion driven MHD generator is limited by the unacceptable low level of the working fluid electrical conductivity at the still rather high temperature of about 2200 - 2300 K. On the other hand the MHD generator inlet temperature is defined mainly by the fuel oxygen mixture in the combustion chamber. The flame temperature for the conditions of a base load power plant is practically not above 3000 K. Hence the temperature interval avalaible for the MHD energy conversion process is strongly limited and the thermodynamic advantages of the MHD generator, as a high temperature device, results to be decreased. The enthalpy extraction in an ideal situation corresponding to the above mentioned temperature range can be not larger than 20 - 25 %.

In order to avoid these limitations an MHD flow with nonuniform plasma structures, hot clots, interacting with the cold surrounding gas has been proposed. The improvement of this type of generator is mainly based on the decrease of the exit temperature to 1700 K at which the MHD conversion process can still be effective. As a consequence a significant growth of the MHD generator efficiency is obtained; the enthalpy extraction is estimated to increase to more than 35 % [6]. The hot clot ($\pm$ 10 % of the flow volume) takes care of the electrical conduction. Consequently the Lorentz force is counteracted by the local pressure gradient mainly generated by the pushing action of the colder gas. In this way the expansion work is delivered by the colder gas. The ohmic dissipation inside the clot provides for a self-sustaining mechanism to keep the clot temperature at a high enough level.

The topic of interest is to define conditions in order to extend the clot lifetime. Therefore the clot behaviour with respect to the self-sustaining mechanism will be analysed by means of experiments with the Eindhoven shock-tube MHD facility and calculations with 1-Dt and 2-Dt codes.

2. THE MODELS USED FOR THE CODES

The codes 'tunotank' and 'FQ2SR' are based on the same numerical model although there are some differences. The mathematical model of the tunotank program is based on a one-dimensional and time-dependent gasdynamical description of the flow [3]. The program simulates the main physical processes taking place in the shock-tube and MHD channel with non-reacting gases. The clot is created by means of a thermal energy pulse and the integral approximation contains an extra thermal energy input factor. The mathematical model of the FQ2SR program is based on a two-dimensional and time-dependent gasdynamical description of the flow simulating the physical processes in the MHD channel with only the test gas [12]. The initial clot is a low density and high temperature area. An extra equation describes the creation of the clot as a change in density of the gas flow at the inlet.

Next sections describe the models used by the tunotank program. The differences with the FQ2SR program will be described further in this report.

2.1 THE MATHEMATICAL MODEL

The classification of the flow equations is connected to the mathematical concept of characteristics which can be defined as families of surfaces in a 3-D unsteady flow along which certain properties remain constant or certain derivates become discontinuous [13,14]. The codes are based on the set of Euler equations which are written in conservative form. The Euler equations form a first order system of non-linear coupled equations. The equations are hyperbolic in time, quantities that propagate along the characteristics can be defined and the equations can be transformed to the characteristic form. The conservative form of the equations (with conservative variables: density, momentum and total energy) is essential in order to compute correctly the propagation speed and the intensity of discontinuities.

The mathematical model used by the tunotank program is based on an one-dimensional and time-dependent description of the flow and an one-dimensional description of the electrodynamical features [3,10]. The time-dependent flow of the chemical non-reacting gas mixture in the presence of body forces is described by the one-dimensional approximation of the Euler equations in the weakly conservative form.

$$\frac{\partial U}{\partial t}+\frac{\partial F}{\partial x}+H=0 \qquad (1)$$

$$U=z(x)\begin{bmatrix}\rho\\ \rho u\\ \rho e_t\\ \rho\alpha_i\end{bmatrix} \qquad F=z(x)\begin{bmatrix}\rho u\\ \rho u^2+p\\ \rho e_t u+up\\ \rho u\alpha_i\end{bmatrix} \qquad H=z(x)\begin{bmatrix}0\\ -p\frac{\partial \ln(z(x))}{\partial x}+j_z B_y\\ uj_z B_y+q\\ 0\end{bmatrix}$$

$i=1,2$	number of mixture component
u	velocity
p	pressure
z(x)	channel cross-section
j_z	electric current density
B_y	magnetic induction
α_i	mass concentration of mixture component
ρ_i	density of mixture component
$\rho=\sum \alpha_i\rho_i$	density
e_i	specific internal energy of mixture component
$e=\sum \alpha_i e_i$	specific internal energy
$e_t=e+u^2/2$	specific total energy
q	thermal energy density per second

The program tunotank uses an extra factor q. The thermal energy density per second q, the region of the thermal energy input, the time instant of switching on the thermal energy pulse and the duration of the thermal energy pulse are input parameters which define the initial clot conditions.

The set of equations is closed by the thermal and caloric equations for the mixture of non-reacting ideal gases:

$$p=\sum_i \frac{\alpha_i}{m_i}\rho RT \tag{3}$$

$$e_i=\int_0^T C_{vi}dT \tag{4}$$

m_i molecular mass of mixture component

C_{vi} heat capacity of mixture component

The considered gas components are He and CO_2.

The electrodynamics of the MHD channel is described with the approximation of ideal Faraday segmentation:

$$k=\frac{R_{load}}{\frac{z(x)}{\sigma y(x)\Delta x}+R_{load}} \tag{5}$$

$$E_z=kuB \tag{6}$$

$$j_y=-\sigma uB(1-k) \tag{7}$$

$$j_x=0 \tag{8}$$

k load factor

Δx segmentation length

z(x) electrode height (channel height)

y(x) electrode width (channel width)

σ electrical conductivity:

$$\sigma=1.83\cdot10^5 T^{\frac{3}{4}} p^{\frac{-1}{2}} e^{\frac{-2.6\cdot10^4}{T}} \tag{9}$$

The ST-MHD facility consists of three different parts: shock-tube, MHD channel and tank. For each region the contour geometry is smooth. The distribution of the gas parameters in the ST-MHD facility before the run is used as an initial condition for the system of the gasdynamic equations. Boundary conditions describe the geometrical peculiarities of the facility construction [3]. The condition of gas reflection and non-penetration is used for the end wall of the shock-tube and the tank. A free stream boundary condition is used for the orifice between channel and tank. A complex boundary condition is used for the end plate between shock-tube and channel, taking into account the gas reflection from the end plate and partial passage of the gas through the orifice of the end plate. This 'rupture transition' boundary condition avarages simultaneous the gas parameters over the interface cross-section.

2.2 THE NUMERICAL METHOD

The FQ2SR and tunotank code are both using a scheme based on the Godunov's-method [6]. Although the Godunov's method for solving compressible flow problems in 2-Dt uses finite difference formulas in rectangular networks their foundation rests on the properties of characteristics of the Euler equations [13,14].

The strong point in Godunov's method is the solution of the problem with respect to the motion of a non-uniformity in a gas flow. The problem can be solved numerically by a method of characteristics employing Riemann invariants. The nonuniform boundary regions are divided into volumes (cells). If the gasdynamical distribution is given at a time-instant we calculate the mean value of the gasdynamic quantities in each cell. The cell interfaces seperate two different fluid states. The evolution of the flow to the next time step results from the wave interactions orginating at the boundaries between cells. The resulting local interaction can be exactly resolved since the initial conditions correspond to the Riemann or shock tube problem of the breakdown at a diaphragm. This problem has an exact solution generally composed of a shock wave, a contact discontinuity and an expansion fan seperating regions of uniform flow conditions. Thus the values of the unknown gasdynamic parameters on each cell boundary are defined and new cell values are determined as the means of values on the left and right boundaries.

The algorithm splits the calculation into time steps and splits for each time step the flow train into cells. The gasdynamic quantities in each cell for each time step are calculated by using the Riemann problem configuration and it's solutions. The flow in the shock-tube, the channel and in the tank is calculated separately. The conjugation of the solutions for the different parts of the flow train is carried out with appropriate boundary conditions as described in chapter 2.1.

The system of the gasdynamic equations (equation 1) is approximated with the finite volume method using the finite difference scheme, an explicit scheme with first order accuracy in time and with second order accuracy in space:

$$U_i^{n+1} = U_i^n - \frac{\Delta t}{\Delta x}(F_{i+1/2}^n - F_{i-1/2}^n) - \Delta t H_i^n \qquad (9)$$

i	- grid node number
n	- number of time layer
i+1/2, i-1/2	- boundaries of control volume
Δt	- time step
Δx	- space step

The volumes (cells) are centered at grid nodes. The numerical fluxes F are considered to be an approximation of the time-averaged physical fluxes at the volume interfaces. The grid node variables U^n_i represent the volume-averaged state variables. The mass, momentum and energy fluxes $F^n_{i\pm 1/2}$ at the volume boundaries are calculated by using the Godunov method. The propagation of the fluxes determines the limitation of the time step; the Courant number. An emperically established procedure decreases the Courant number when the MHD interaction is high.

One of the important features of the non-uniform gas flow is the strong influence of the processes in the relatively small hot clot on the total flow structure. The dynamic interaction between hot and cold gas can produce a complicated non-steady state shock wave pattern. Therefore the numerical method should provide high accuracy in the description of strong gradient regions and discontinuities in the flow. The consideration of the numerical solution showed that Godunov's method, supposing constant distributions of gasdynamical parameters inside cells, doesn't ensure good description of the flow regions with strong gasdynamical gradients.

The situation with high temperature clots will cause non-physical increment of gasdynamical gradients. To prevent this situation the Godunov-Kolgan method is used with second order space accuracy instead of piecewise constant distributions inside the cells [6,8].

A specific numerical procedure, a quasi-Lagrange approach, has been developed to reach a high resolution of the clots [6]. The quasi-Lagrange algorithm has been realized on the base of the Godunov's scheme. Cells move locally with the gas velocity, calculated as the velocity of the contact surface occuring in the Riemann problem configuration. The flux of mass through the cell border is excluded automatically and the numerical spreading up of contact discontinuities is absent (clots will be impermeable for the hot gas).

The scheme provides monotonic profiles of gasdynamical parameters and spreading of contact discontinuities (temperature discontinuities) and shock waves (pressure discontinuities) over several cells.

3. THE TUNOTANK PROGRAM

The tunotank program calculates the main physical processes taking place in the Eindhoven shock-tube MHD facility. The mathematical modelling of these processes is based on a one-dimensional and time-dependent gasdynamical description of non-reacting gases by Euler equations averaged in y- and z-direction, an one-dimensional description of the electrodynamical features and an integral model to describe the generation of the nonuniformities [10]. Several probes positioned along the x-axis of the configuration 'measure': static pressure, static temperature, density and electrode voltage in time. The configuration of the shock-tube and MHD channel facility is presented in figure 3.1. The geometry in y-direction is the same as in z-direction; $y(x) = z(x)$. The input parameters for the tunotank program are:

DRIVER and TEST SECTION

- Initial temperature of driver and test gas.
- Initial pressure of driver and test gas.
- Specific heat ratio of driver and test gas.
- Moleculair weight of driver and test gas.

DIAPHRAGM SECTION

- Initial pressure.

HEAT INPUT SYSTEM

- Upstream location of the thermal energy pulse.
- Downstream location of the thermal energy pulse.
- Time instant of switching on the thermal energy pulse.
- Duration of the thermal energy pulse.
- The thermal energy density per second.

MHD SYSTEM

- Amount of electrode pairs: 81
- Location of electrode pairs: 0.38 m - 1.18 m
- Segmentation length: 1 cm
- Electrode width: y(x)
- Electrode height: z(x)
- Load resistance: 5 Ω
- Magnetic induction.

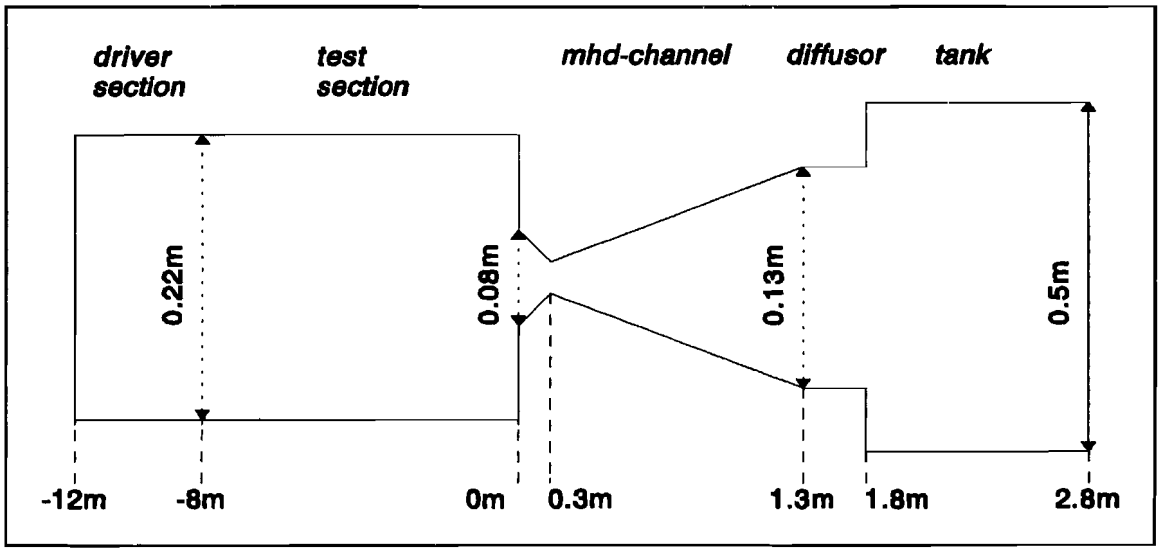

Figure 3.1 The Eindhoven shock-tube and MHD channel facility.

3.1 THE TUNOTANK SIMULATIONS WITHOUT CLOT

The program considers constant heat capacities for the non-reacting ideal gases. An appropriate value for the heat capacity of the test gas CO_2 at $T = 2000$ K is distracted (appendix A). The standard initial conditions for the shock-tube are:

Driver section [He]
$T = 290$ K, $p = 1.1 \cdot 10^6$ Pa, $\gamma = 1.67$
Test section [CO_2]
$T = 1100$ K, $p = 8 \cdot 10^3$ Pa, $\gamma = 1.16$

To analyse the gas flow development probes are positioned in the shock tube at -0.5 m and -0.01 m (just upstream of the end plate) and in the MHD channel at 0.01 m (just downstream of the end plate). Figure 3.2 presents the wave propagation diagram. Figure 3.3 shows the pressure plots. After the breakdown of the diaphragm the incident shock wave and the rarefaction waves divided by the contact discontinuity propagate in the shock tube (a). After the incident shock wave has reached the end of the tube it partly passes into the MHD channel and partly reflects against the end plate (b). Because of a grid length of 2 cm in the shock tube, the probe at -0.01 m 'measures' the process at the end plate. Almost a motionless region of compressed test gas with high pressure and temperature will exist between the end plate and the reflected shock wave, the stagnation region, which expands through the end plate (c). At a certain distance from the end plate the reflected shock wave interacts with the contact discontinuity (d) and a compression wave propagates to the end plate and destroyes the stagnation region after which the Helium bulk flow follows (e). The Helium flow partly reflects against the end plate and partly propagates into the MHD channel (f). Figure 3.4 shows the quasi-stationary area, situated between the incident shock wave and the Helium bulk flow, moving along the MHD channel. This area expands because of different velocities of the incident shock wave and the Helium flow. The clot will be created in this quasi-stationary area of the gas flow to extend the clot lifetime.

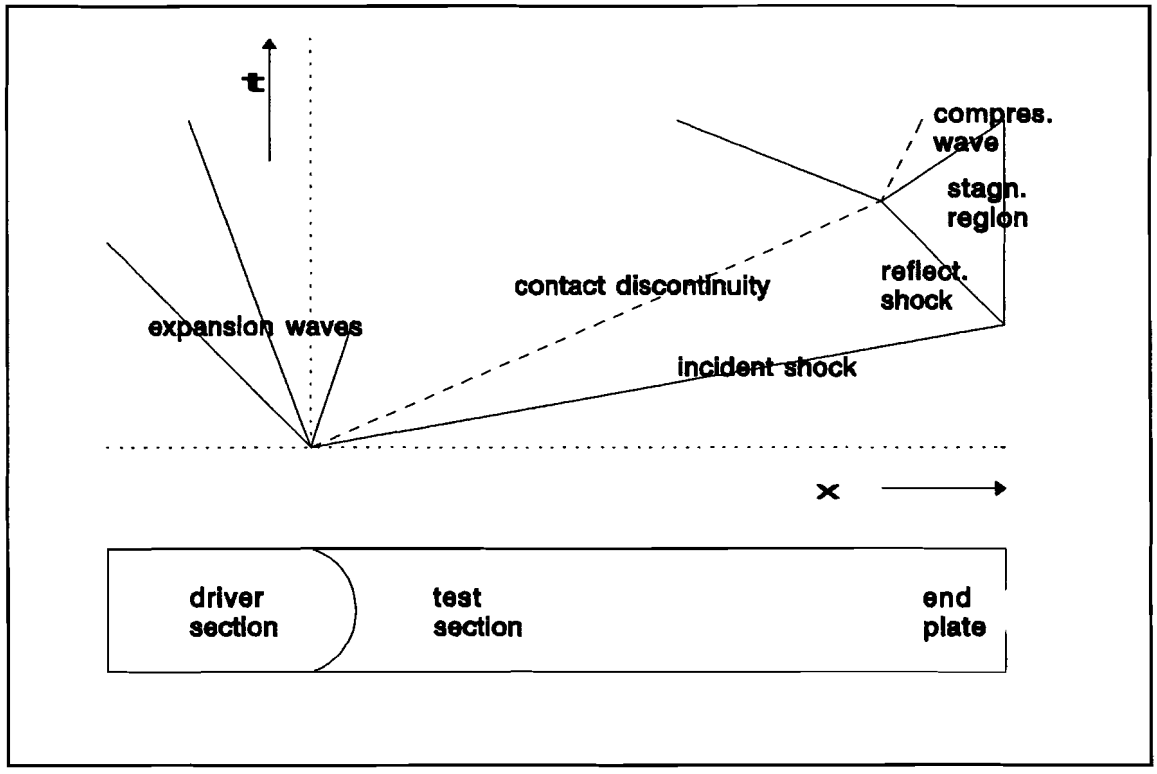

Figure 3.2 The wave propagation diagram for the shock-tube.

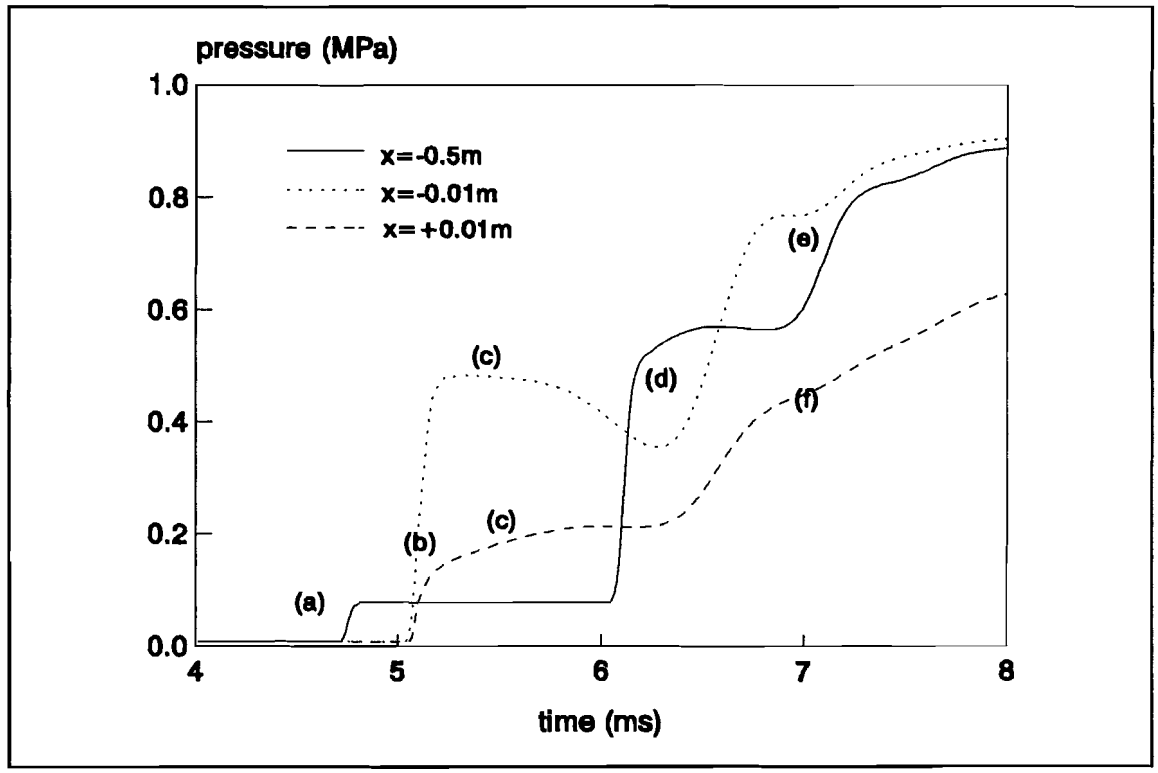

Figure 3.3 The reflection of the pressure waves from the end plate in the shock-tube and the propagation through the orifice of the end plate into the MHD channel.

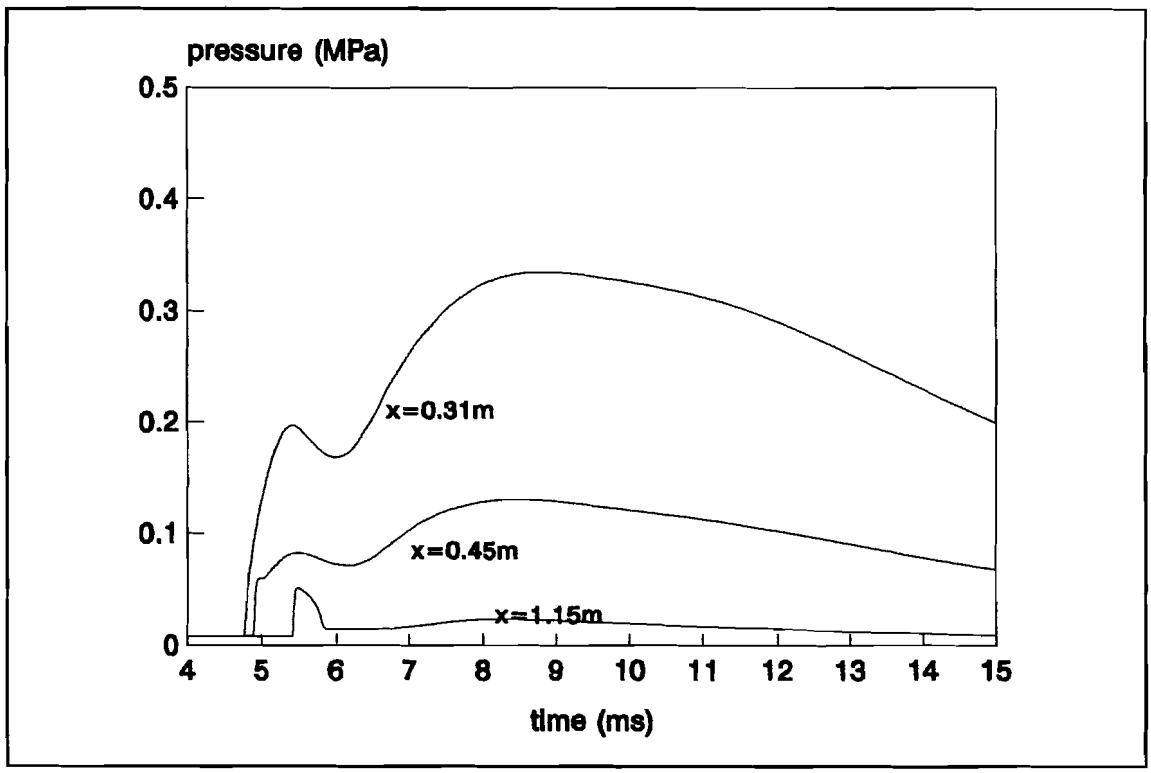

Figure 3.4 The pressure waves propagation in the MHD channel.

3.2 THE TUNOTANK SIMULATIONS WITH CLOT

The high temperature conducting clots are generated by short pulse heating of the gas flow. The clots are defined by the following input parameters: density of the thermal energy supply, time duration of the thermal energy supply and size and position of the region of the thermal energy supply. The clots are formed in the beginning of the MHD channel just after the nozzle to examine the passage of the clot through the whole channel. The following set of input parameters is used to define the standard clot conditions which are resp. an initial clot temperature of 3500 K and an initial clot size of 10 cm.

HEAT INPUT SYSTEM

Region of thermal energy pulse:	$x = 0.36$ m - $x = 0.46$ m.
Start thermal energy pulse:	$t = 6.6$ ms.
Duration of thermal energy pulse:	1 μs.
Thermal energy density per second:	$30 \cdot 10^{10}$ J/m^{3}s.

Figure 3.5 shows the position of the standard clot with regard to the quasi-stationary area. Probes are positioned at (1) $x = 0.46$ m, (2) $x = 0.69$ m, (3) $x = 0.92$ m and (4) $x = 1.15$ m. The temperature and pressure of the quasi-stationary area when it passes the nozzle are resp. 2500 K and 0.17 MPa.

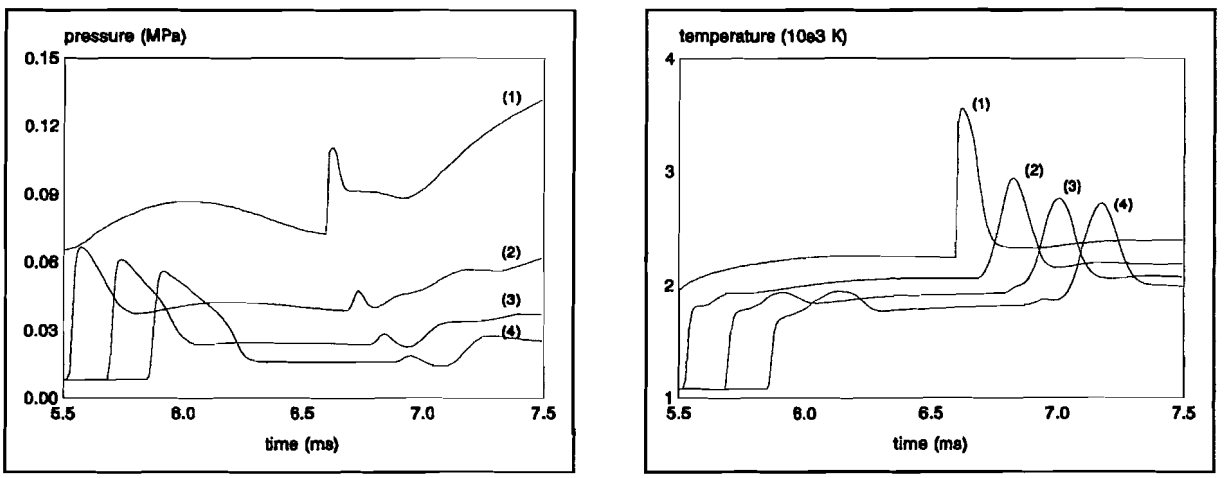

Figure 3.5 The clot position with respect to the quasi-stationary area at successive probe locations.

Simulations have been done for different conditions (the gas temperature as mentioned below is the temperature of the quasi-steady state area when it passes the nozzle):

- Gas temperature: 1500 K, 2000 K, 2500 K and 3000 K.
- Magnetic induction: 1.5 T, 2.5 T and 5 T.
- Initial clot size: 5 cm, 10 cm and 15 cm.
- Voltage drop: yes/ no.
- Plasma conductivity: low/ high.

The standard conditions are:

temperature gas (K)	magnetic induction (T)	initial clot size (cm)	voltage drop	plasma conductivity
2500	2.5	10	no	high

Four probes are positioned every 23 cm along the MHD channel x-axis at (1) x = 0.46 m, (2) x = 0.69 m, (3) x = 0.92 m and (4) x = 1.15 m (figure 3.6).

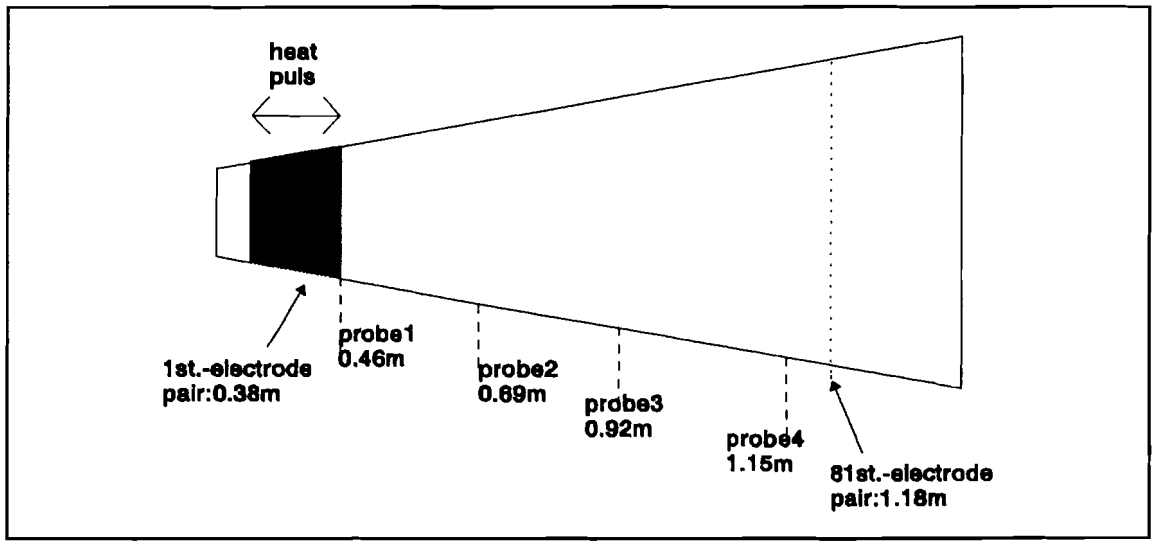

Figure 3.6 The MHD channel configuration.

The probes 'measure': pressure, temperature, density and electrode voltage in time. The maximum 'measured' clot temperature, pressure and electrode voltage are used for calculating the plasma resistance and velocity in the 'hot' clot center. The load factor calculation is based on the plasma resistance in the clot center.

$$\sigma = \sigma_0 T^{\frac{3}{4}} p^{-\frac{1}{2}} e^{\frac{-2.6 \cdot 10^4}{T}} \tag{1}$$

$$R_{plasma} = \frac{z(x)}{y(x)\sigma\Delta x} \tag{2}$$

$$u_{clot} = \frac{V}{y(x)B}\left(1 + \frac{R_{plasma} + R_{boundary}}{R_{load}}\right) \tag{3}$$

$$k = \frac{R_{load}}{R_{plasma} + R_{boundary} + R_{load}} = \frac{1}{1 + \frac{P_{diss}}{P_{el}}} \tag{4}$$

- $\sigma_0 = 1.85 \cdot 10^5$ for the condition with high plasma conductivity.
  $\sigma_0 = 1.85 \cdot 10^4$ for the condition with low plasma conductivity.
- $R_{boundary} = 0$ for the condition without voltage drop.
  $R_{boundary} = 195\ \Omega$ for the condition with voltage drop.
- $R_{load} = 5\ \Omega$.
- The segmentation length, Δx, is 1 cm. The electrode height, channel height z(x), is equal to the electrode width, channel width y(x).

The half-width of the clot temperature plot indicates the clot passing time for each probe. The clot size, when the clot passes the probe, is calculated by multiplying the clot velocity with the clot passing time.

3.3 RESULTS OF THE TUNOTANK SIMULATIONS

THE STANDARD CONDITIONS

The clot is created by a thermal energy pulse which means that the clot is a high pressure and high temperature area. The program doesn't consider heat conduction, heat radiation and diffusion which means that the clot temperature is decreasing due to clot expansion. The clot dimensions in y- and z-direction are equal to the channel dimensions because of uniform conditions in these directions. The clot expansion follows the gas flow expansion. Clot expansion in x-direction takes place because of the pressure gradient between clot and gas (figure 3.7). The pressure gradient within the clot is mainly negative.

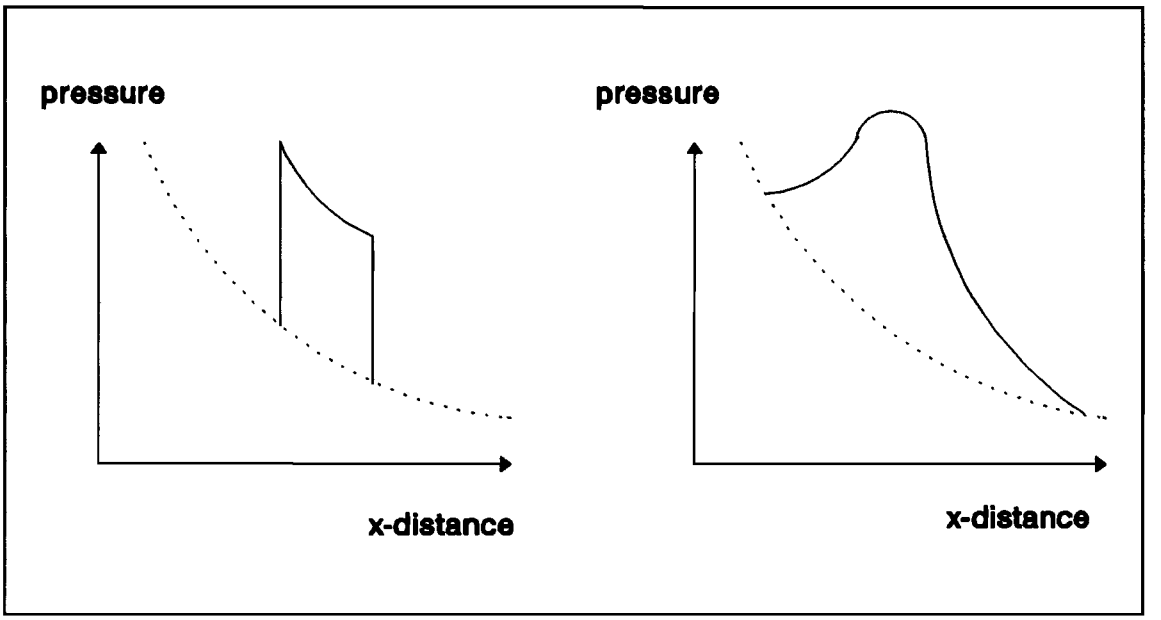

Figure 3.7 The clot deformation due to expansion in y- and z-direction (left) and in x-direction (right).

Figure 3.8 shows that pressure waves propagate upstream and downstream from the clot due to the pressure gradient between clot and gas.

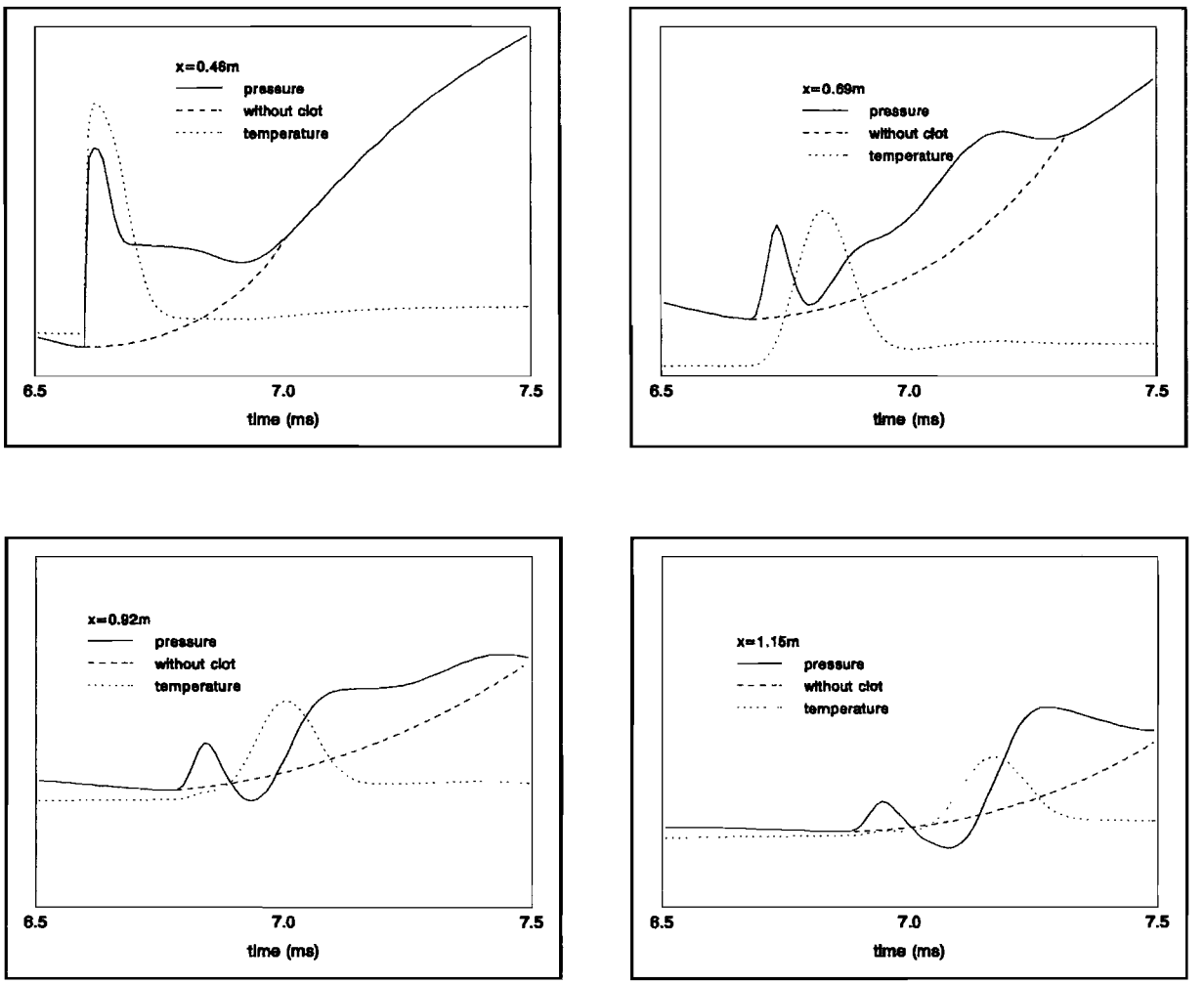

Figure 3.8 The pressure inside the clot and upstream and downstream of the clot with respect to the situation without the clot at successive probe locations.

When the clot moves along the channel the clot temperature decreases and the clot plasma resistance increases (figure 3.15). The clot current increases (figure 3.16). The load factor decreases due to a stronger increment of the internal dissipation compared with the electrical power increment (figure 3.14 and equation 4). For the condition without magnetic interaction the clot temperature decreases faster due to absence of the internal dissipation (figure 3.9).

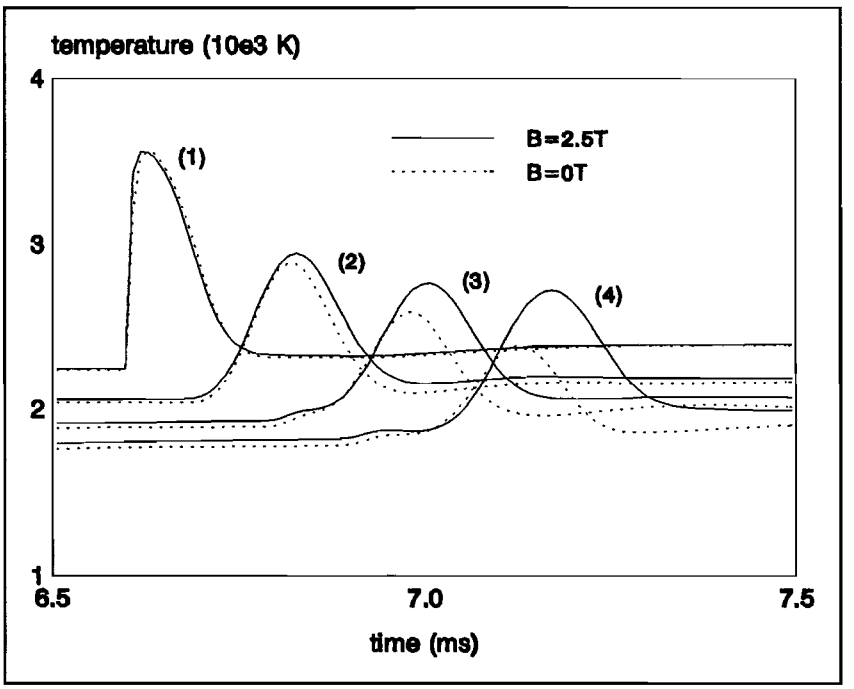

Figure 3.9 The temperature with and without magnetic interaction at successive probe locations.

Figure 3.10 shows the gas pressure increment upstream of the clot because of clot deceleration due to magnetic interaction.

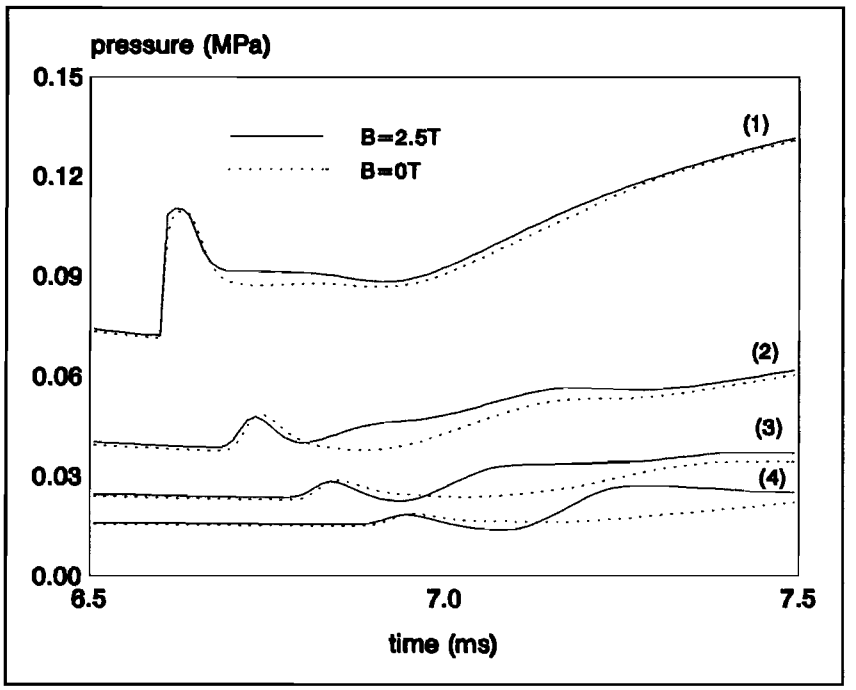

Figure 3.10 The pressure with and without magnetic interaction at successive probe locations.

The clot deforms from a rectangular to a more smooth geometry due to expansion. The current and the dissipation are concentrated in the clot area with the highest temperature which causes a deformation of the clot (figure 3.11). The passing time (the time required to pass a probe) is derived from the half-width of the clot temperature plot. The passing time of a high temperature clot is shorter than for a low temperature clot. Calculating the clot size, by multiplying the clot velocity with the passing time, results in smaller values for high temperature clots. This explains the lower axial clot size increment when magnetic interaction is present (figure 3.18).

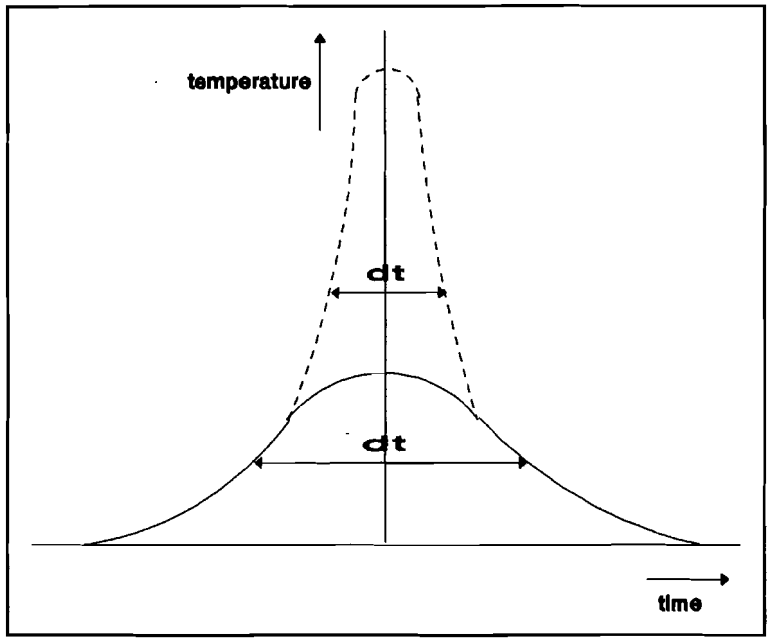

Figure 3.11 The passing time for a high and low temperature clot at a probe location.

PARAMETER: MAGNETIC FIELD

High magnetic field causes high current and deceleration of the clot (figure 3.15 and 3.17). The clot temperature is stable for B = 5 T. For this condition the clot pressure and temperature remain high due to the internal dissipation. Because of the deceleration of the clot the gas pressure before the clot increases which counteracts the upstream clot expansion. The load factor for B = 5 T remains high (figure 3.14) which indicates a strong electrical power increment. The Lorentz-force, internal dissipation and electrical output power are proportional to B^2 which explains the high magnetic interaction for B = 5 T:

$$F_l = \oint_{V_{clot}} \sigma u B^2 (1-k) dV \qquad (1)$$

$$P_{diss} = \oint_{V_{clot}} \sigma (uB)^2 (1-k)^2 dV \qquad (2)$$

$$P_{el} = R_{load} \oint_{A_{clot}} \sigma^2 (uB)^2 (1-k)^2 dA \qquad (3)$$

PARAMETER: GAS TEMPERATURE

Next values are used for the temperature of the quasi-stationary area when it passes the nozzle: 1500 K, 2000 K, 2500 K and 3000 K. The gas temperature is defined by the initial shock-tube settings. Higher gas temperature also means higher gas velocity and induced field (uB). Lower gas temperature means a pulse with higher thermal energy density per second to create a clot with the same initial clot temperature (3500 K). More thermal energy means a higher initial pressure gradient between clot and gas, resulting in more clot expansion and more decrease of clot temperature (figure 3.15 and 3.18).

The clot current decreases and the clot velocity (figure 3.17) follows the gas velocity (appendix B) due to the low magnetic interaction. Lower clot temperature causes electrode voltage decrement (figure 3.16):

$$V = \frac{R_{load}}{R_{plasma} + R_{load}} \cdot uBz \qquad (4)$$

The load factor, the clot temperature, the electrode voltage and the internal dissipation remain high for the conditions of Tgas = 2500 and 3000 K. Decreasing the gas temperature results in a strong decay of the clot.

PARAMETER: VOLTAGE DROP

A boundary resistance of 195 Ω accounts for a voltage drop in the channel. The clot temperature development corresponds with the condition without magnetic interaction. Apparently the current is too small to cause substantial internal dissipation. The Lorentz-force is negligible and the clot velocity is almost equal to the gas velocity. The energy is dissipated in the boundary resistance; the load factor is almost zero (figure 3.14).

PARAMETER: THE PLASMA CONDUCTIVITY

The program is using a constant σ_0 in the calculation of the plasma conductivity (equation 1 page 5). To account for lower plasma conductivity, the σ_0 is decreased with a factor 10. For this condition the clot current is low (figure 3.16) and the clot velocity follows the gas velocity. The load factor is decreasing fast (figure 3.14), the energy is dissipated in the plasma. The plasma resistance is high and the internal dissipation provides for less decrease in clot temperature (figure 3.15).

Parametervalues for the initial clot size are; 5 cm, 10 cm and 15 cm. The clot temperature and electrode voltage development for the condition of large initial clot size (15 cm) corresponds to the condition of standard initial clot size (figure 3.15 and 3.16). The load factor is high (figure 3.14) and the clot current increases along the channel, the internal dissipation causes less decrease of clot temperature. For the condition of small initial clot size the load factor, clot temperature and current are decreasing along the channel. The pressure gradient between clot and gas is higher for small clots and expansion waves destroys the clot earlier (figure 3.12).

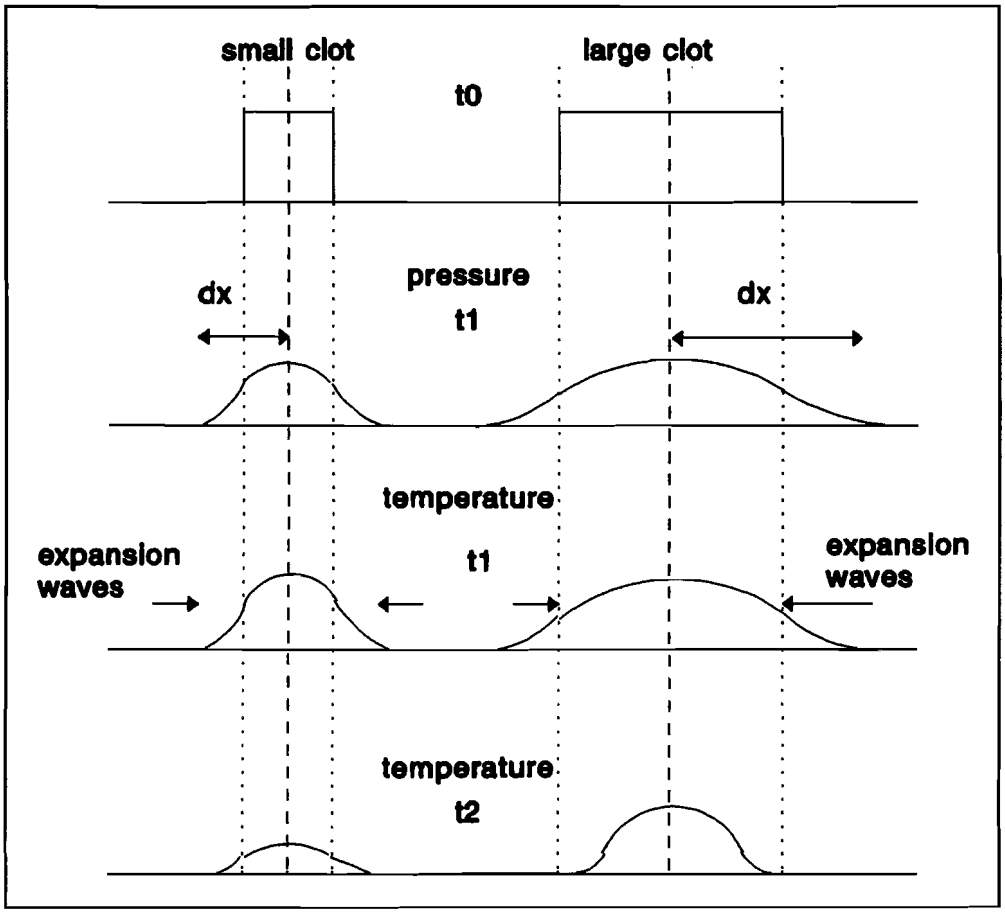

Figure 3.12 The pressure and temperature for small and large clots at successive time instants.

The program calculates the electrical output energy and the input energy needed to create the clot. The input energy is calculated by multiplying the thermal energy density per second with the duration of the thermal energy supply and with the channel volume where the supply takes place. Figure 3.13 shows for the condition of high magnetic field (5T) higher electrical output energy than input energy. The electrical power output is higher and the magnetic interaction is high enough to extend the clot lifetime because the electrical power output and the internal dissipation are both proportional to B^2 (equation 6 and 7).

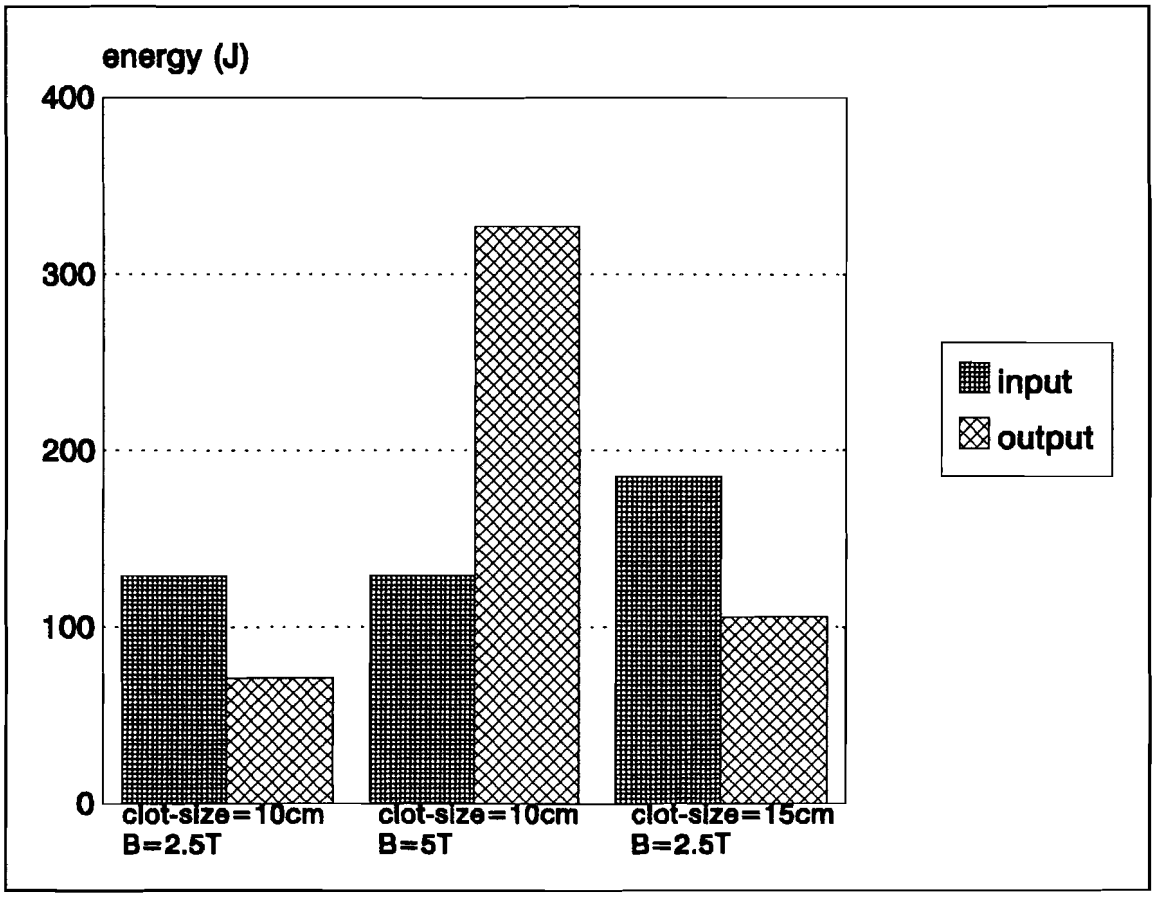

Figure 3.13 The thermal input energy and electrical output energy for different conditions.

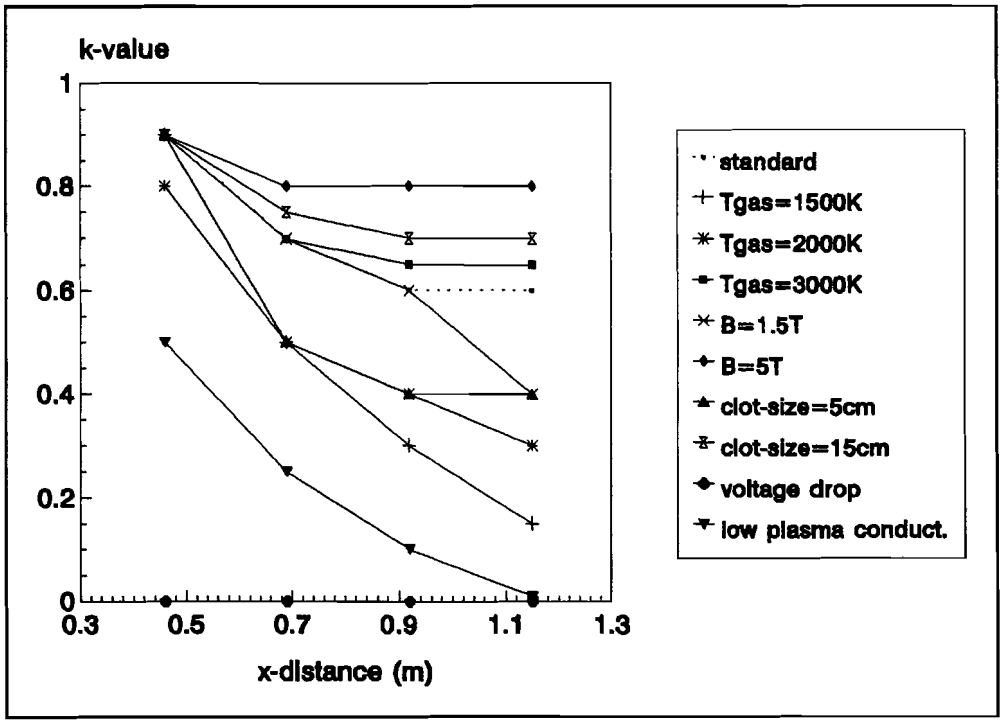

Figure 3.14 The load factor along the x-axis for different conditions.

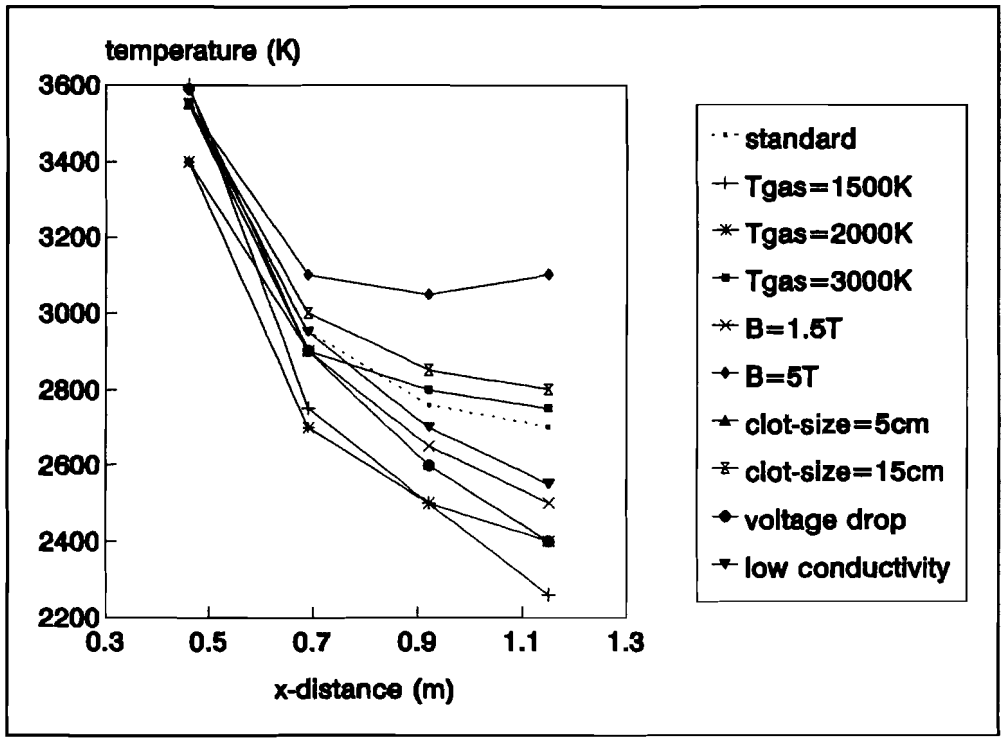

Figure 3.15 The maximum clot temperature along the x-axis for different conditions (the initial clot temperature is about 3500 K).

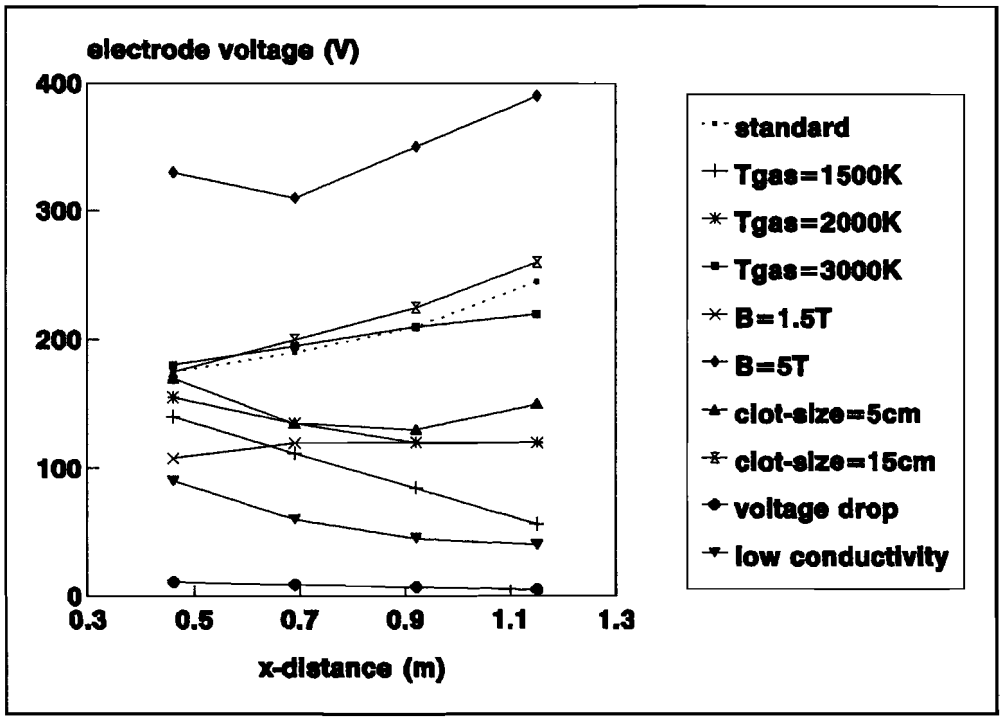

Figure 3.16 The maximum electrode voltage along the x-axis for different conditions.

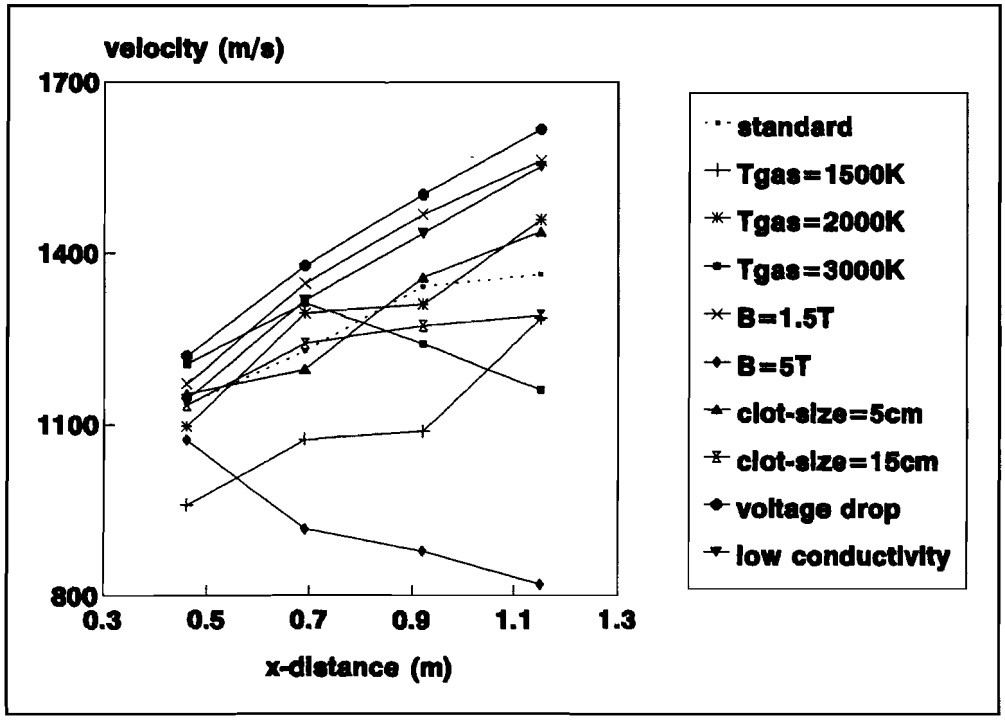

Figure 3.17 The clot velocity along the x-axis for different conditions.

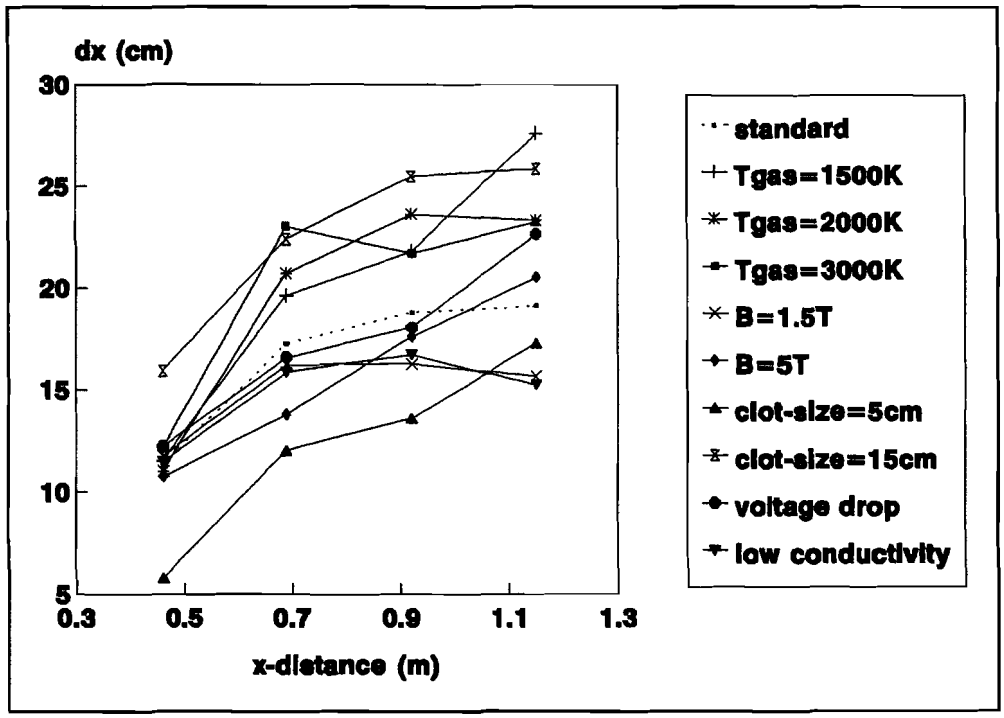

Figure 3.18 The axial clot size along the x-axis for different conditions.

4. THE FQ2SR PROGRAM

The code FQ2SR is based on a quasi two-dimensional time dependent model of the fluid flow [6]. The directions of study are the x-direction which is the direction of the flow and the y-direction which is the direction of magnetic induction. It describes the evolution of the flow in a Faraday type ideally segmented MHD channel with the following assumptions:

- No viscosity, thermal conduction, turbulence, diffusion and boundary layers.
- Ideal gas approximation.
- Clots are impermeable for the cold gas.
- Stationary inlet conditions.
- Uniform conditions in the z-direction.
- Only MHD interaction in the clot.
- Different regions:
  an inlet region without divergence in which a clot is formed,
  a working zone in which magnetic induction is present and
  current is collected.
- No divergence in y-direction; the magnetic field direction. Divergence is present in the z-direction which is the electric field direction.

The results of the code are the distribution of the gasdynamic quantities (pressure, temperature and x-component of velocity) in the x-y-plane and the enthalpy extraction at time instants which are choosen at the startup of the simulation.

The following set of values is used for input data (figure 4.1):

1. CHANNEL GEOMETRY
   - L (channel length)
   - a (dimension in the y-direction)
   - z(x) (dimension in the z-direction)

2. INLET CONDITIONS
   - p_0 (inlet pressure)
   - u_0 (inlet x-component of velocity;no w_0 inlet y-component)
   - ρ_{0c} (inlet density of the cold gas)
   - ρ_{0h} (density of the hot clot at time of formation)

4. CLOT GEOMETRY
   - a_h (dimension of the clot in y-direction at time of formation)
   - τ_h ($\tau_h u_0$ the dimension of the clot in the x-direction at time of formation)

5. LOAD CONDITIONS
   - $B_y(x)$ (magnetic induction along the x-axis in y-direction)
   - E_z (electric field along the x-axis in z-direction)

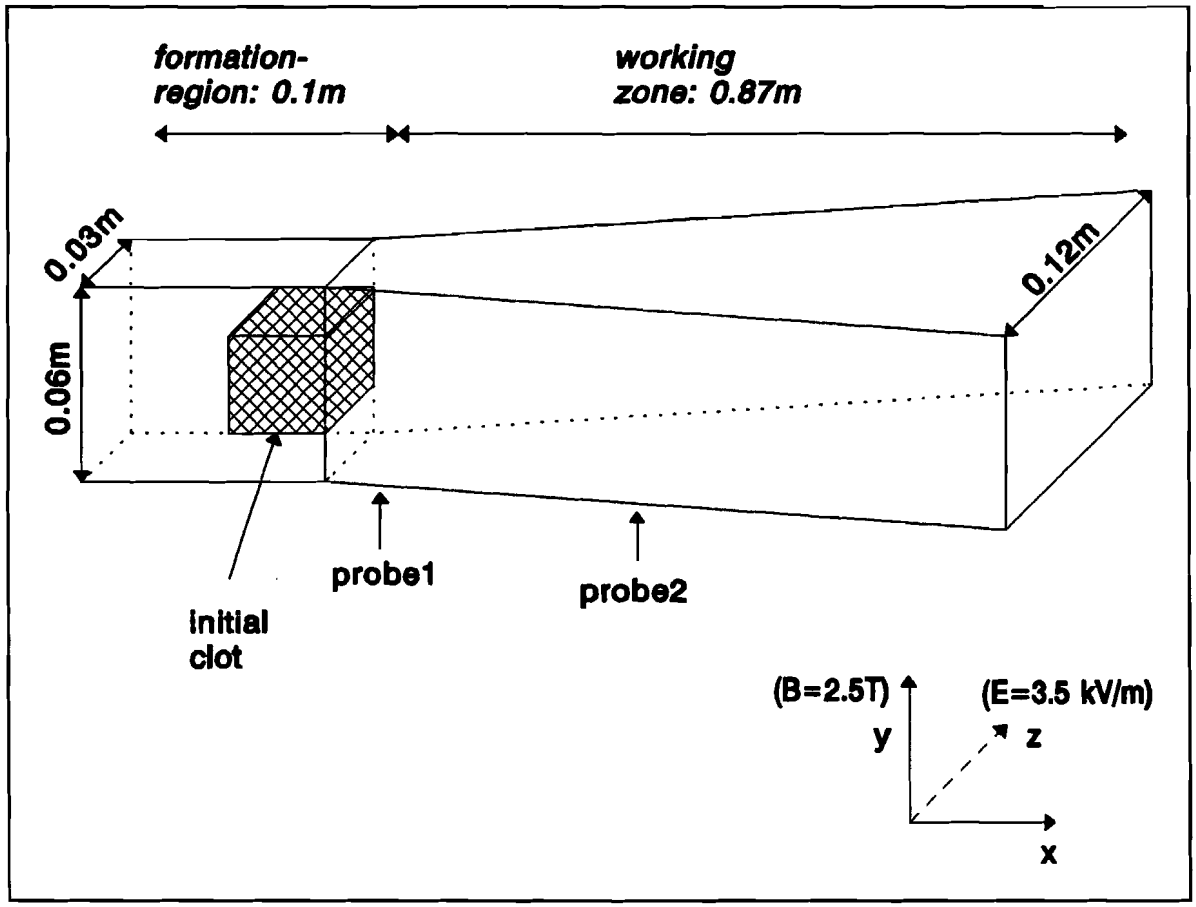

Figure 4.1 The MHD channel configuration.

The flow in the MHD channel consists of a cold non-conducting gas and a hot high conducting gas. The initial gasdynamic conditions correspond to the steady state supersonic flow of cold gas without a clot through the channel. For $t>0$ the hot gas clot is being introduced into the channel inlet (figure 4.1). The velocity u_h and static pressure p_h of the hot gas are equal to the corresponding parameters of the cold gas. The density ρ_h of the hot gas is different from ρ_c of the cold gas. The initial shape of the hot gas clot is like a brick moving along the channel axis. It's initial y-dimension is a_h. It's z-dimension during the process is equal to the channel dimension z(x). It's initial x-dimension is $\tau_h u_0$.

The equations used for the code are 2-D time-dependent Euler's equations averaged in the z-direction (chapter 2.1). To visualize the flow structure and to define the position of the clot an auxiliary equation for the marker ξ is solved:

$$\frac{\partial z(x)\rho\xi}{\partial t}+\frac{\partial z(x)\rho u\xi}{\partial x}+\frac{\partial z(x)\rho w\xi}{\partial y}=0 \qquad (1)$$

The gasdynamical boundary conditions at the left boundary of the calculation region are assigned in the form:

$u(0,t)=u_0$, $p(0,t)=p_0$,

if $0< t <\tau_h$ then

$\rho(0,t)=\rho_{0h}$, $\xi(0,t)=1$

and for $t>\tau_h$

$\rho(0,t)=\rho_{0c}$, $\xi(0,t)=0$.

The gas flow has a supersonic character although the inlet Mach number of the clot may be less then 1. In the entrance section disturbing factors are absent. The boundary conditions at the wall $y=a$ and the centerline plane $y=0$ is that $w=0$ (the y-component of velocity). Due to symmetry of the problem only the half-width of the channel is considered. The performance of the channel is given by the enthalpy extraction; stagnation values are used. The enthalpy extraction coefficient is defined as:

$$\eta_{ent}=\frac{P_{el}}{(\dot{m}H)_{inl}}=\frac{-\int_{V_{clot}} E_z j_z dV}{\frac{\gamma}{\gamma-1}R\left(\int_{A_{inlet}}\rho u T_s dA\right)} \qquad (2)$$

Because of equal values of the velocity and pressure for the clot and the gas at the inlet, the enthalpy of the inlet gas flow is constant during the process.

4.1 THE FQ2SR SIMULATIONS

The code uses a constant specific heat ratio of 1.25. The channel geometry is presented in figure 4.1. Further input data:

GEOMETRY OF THE WORKING ZONE

- amount of electrode pairs: 87
- segmentation length: 0.01 m
- electrode width: 0.06 m
- electrode height: z(x)

INLET CONDITIONS

- static pressure: 4.44 bar (stagn.pres.: 8 bar)
- static temperature: 3100 K (stagn.temp.: 3500 K)
- velocity: 1090 m/s

LOAD CONDITIONS

- magnetic induction: 2.5 T in working zone (constant)
- electric field: 3.5 kV/m in working zone (constant)

POSITION OF PROBES

- x: 0.225 m
- x: 0.495 m

The initial clot-temperature is 3500 K or 4100 K (stagnation values: 3900 K or 4500 K). The initial clot-dimensions are:

dx: 2.5 cm dy: 2.5 cm	dx: 2.5 cm dy: 5.0 cm	dx: 5.0 cm dy: 2.5 cm	dx: 5.0 cm dy: 5.0 cm	dx: 10 cm dy: 5.0 cm

4.2 RESULTS OF THE FQ2SR SIMULATIONS

Analysing the conditions at the channel inlet it appears that the electric field is higher than the induced field (uB), the enthalpy extraction coefficient is negative and electric energy is supplied to the clot. The enthalpy extraction coefficient plots show that the duration of negative enthalpy extraction coefficient is less than 50 μs. The MHD interaction is proportional to the value of the enthalpy extraction coefficient:

$$uBz(x)I = \frac{1}{k} P_{el} = \frac{uB}{E} (\dot{m}H)_{inl} \eta_{enth} \qquad (3)$$

During the first 50 μs of the simulation the clot velocity is low. Therefore the results of the calculations for the (short) period of negative enthalpy extraction coefficient are neglected.

OPTIMALISATION

Figure 4.2 and 4.3 present the enthalpy extraction coeffients in time.

- Clots with high initial temperature and large size appear to have a longer lifetime and cause a higher enthalpy extraction coefficient.
- The enthalpy extraction coefficient ratio is calculated when the initial x- or y-dimension of the clot is doubled (appendix C). It appears that: (1) increasing the initial x-dimension of the clot causes a higher increment in the enthalpy extraction coefficient ratio than increasing the initial y-dimension, particularly for high initial clot temperature, (2) increasing the initial clot surface four times causes more than two times increase of the enthalpy extraction coefficient ratio, particularly for high initial clot temperature.
- Increasing the initial clot temperature from 3500 to 4100 K causes the highest increase in the enthalpy extraction coefficient ratio for large clots (appendix C).
- Increasing the initial clot temperature causes more enthalpy extraction coefficient ratio increment than increasing the initial clot dimensions.

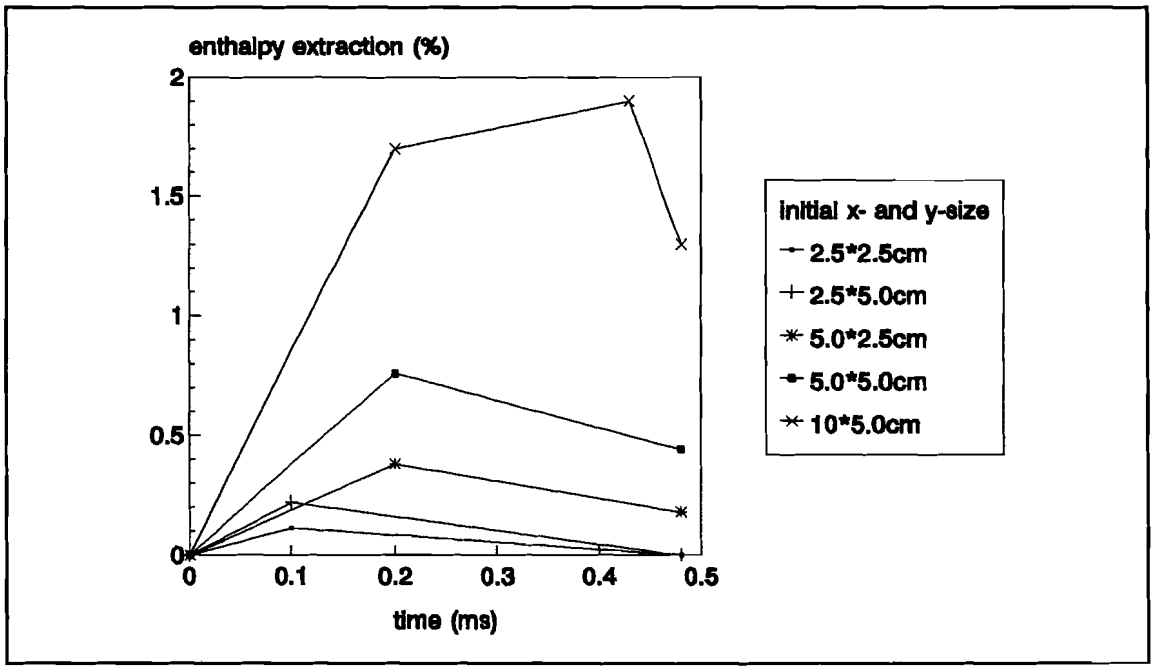

Figure 4.2 The enthalpy extraction coefficient for high initial temperature clots (4100 K).

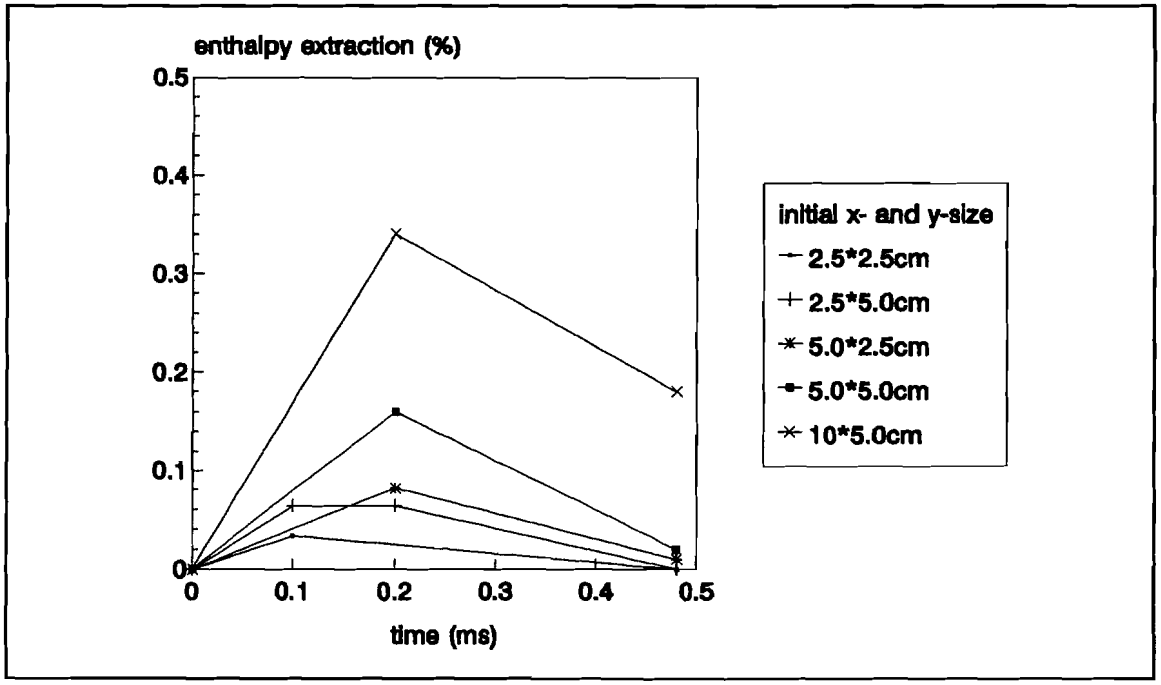

Figure 4.3 The enthalpy extraction coefficient for low initial temperature clots (3500 K)

The current vs. time plots for the two probes are used to calculate the passing time by deriving the half-width. Multiplying the passing time with the clot velocity gives the clot size in x-direction. Velocity plots show that the difference between clot and gas velocity is max. 5 % for conditions of high initial clot temperature. To calculate the clot x-size, the clot velocity is supposed to be equal to the gas velocity (appendix c). The clot geometry changes along the channel due to concentration of dissipation in the clot area with the highest temperature and results in smaller values of the axial clot size for high temperature clots as explained in chapter 3.3 (p. 21).

The clot temperature is decreasing due to expansion of the clot. Because of the quasi two-dimensional numerical model of the fluid flow, uniform conditions are considered in z-direction. The clot size in z-direction is equal to z(x), the channel height, and the clot expansion in z-direction can be compared with the gas flow expansion (figure 4.4). Figure 4.5 shows two regions of clot temperature decay; in the first half of the channel the temperature gradient is more intense than in the second half of the channel. Clot expansion in x- and y-direction takes place when a pressure gradient between clot and gas is present caused by internal dissipation.

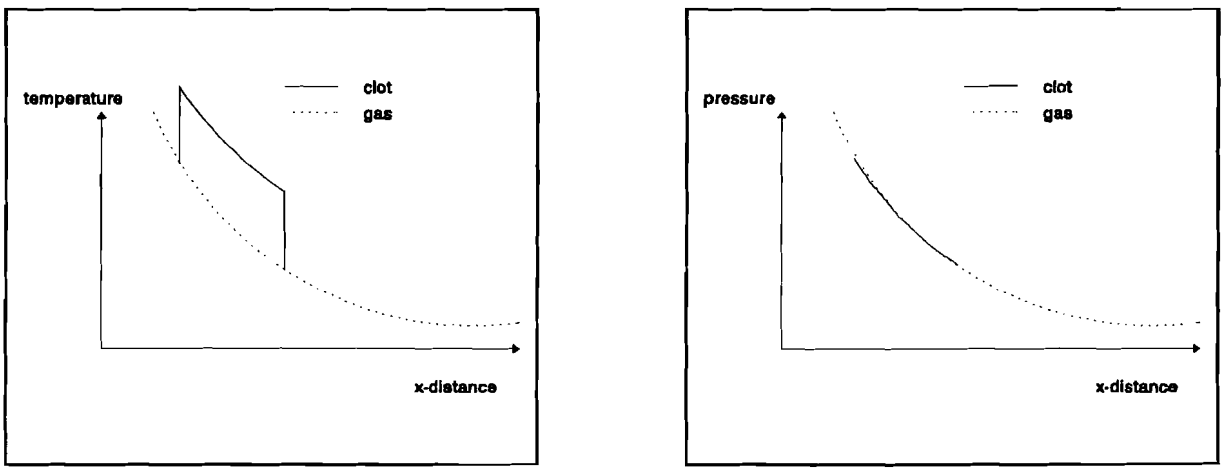

Figure 4.4 The clot temperature and pressure decay due to expansion in z-direction.

Higher initial clot temperature (higher conductivity) or larger initial dimensions causes more internal dissipation (equation 5). A second effect is the increase of the Lorentz-force (equation 4) which causes deceleration of the clot. Increasing the initial clot temperature causes a higher increment in clot current (figure 4.6) and Lorentz-force than increasing the initial clot dimensions. The enthalpy extraction coefficient plots confirm that the Lorentz-force is higher for high temperature clots (figure 4.2 and 4.3). The Lorentz-force is proportional to the enthalpy extraction coefficient and the enthalpy extraction coefficient is higher for high temperature clots:

$$F_l = B \int_{V_{clot}} \sigma(E - uB)dV = \frac{B}{E}(\dot{m}H)_{inl}\eta_{enth} \tag{4}$$

$$P_{diss} = \int_{V_{clot}} \sigma(E - uB)^2 dV \tag{5}$$

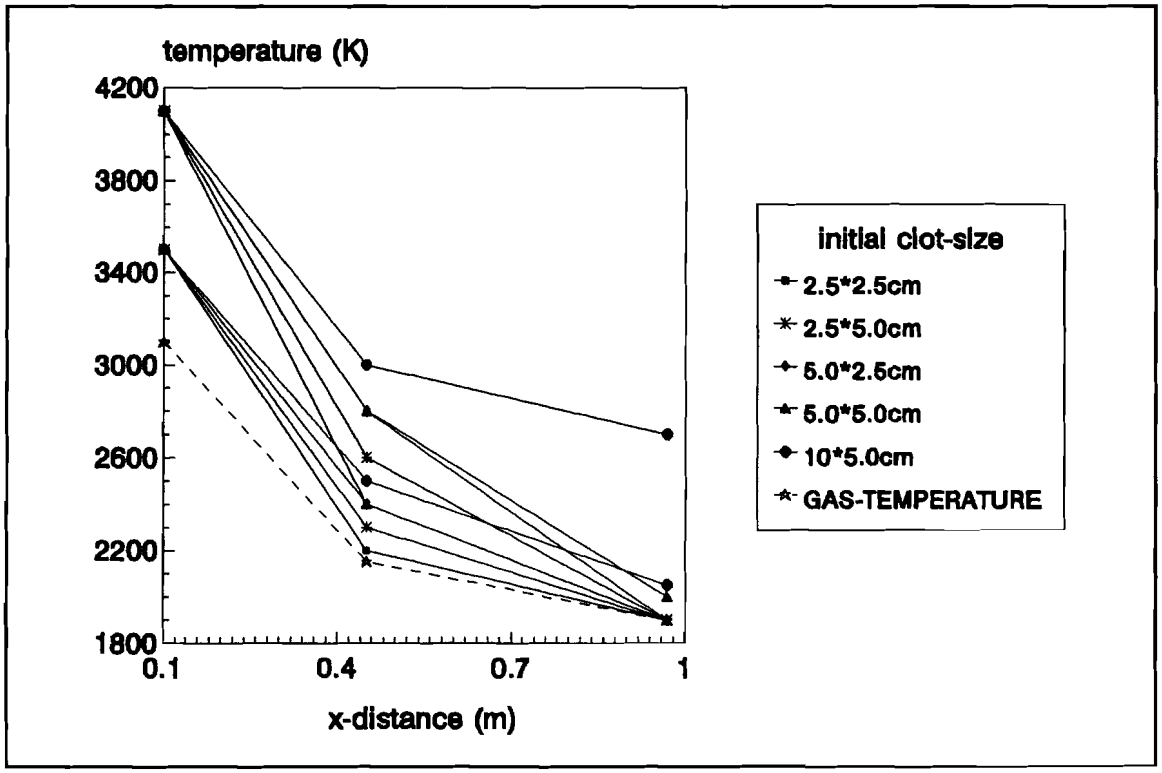

Figure 4.5 The maximum clot temperature along the x-axis.

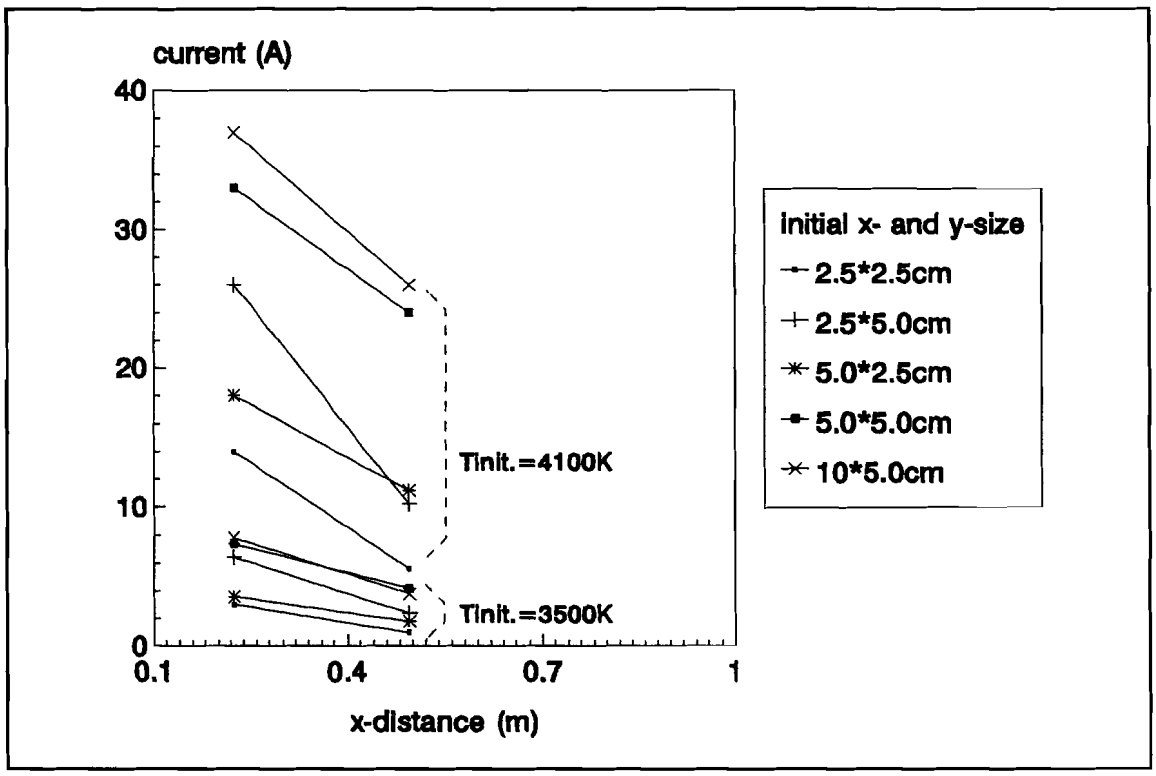

Figure 4.6 The maximum clot current along the x-axis.

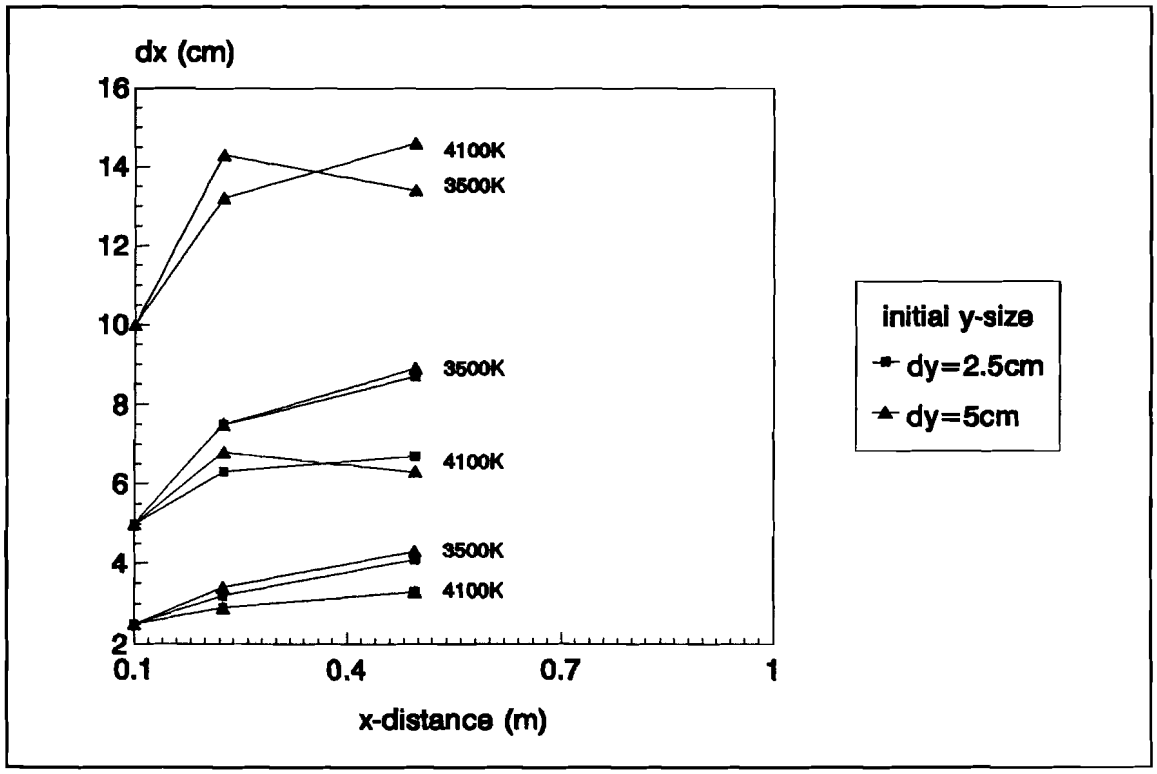

Figure 4.7 The axial clot size along the x-axis.

The clot decelerates due to the Lorentz-force and interacts with the pushing gas flow. The clot disturbs the gas flow resulting in a pressure gradient in y-direction between clot and gas flow. The clot deforms and expands in y-direction (figure 4.8). The enthalpy extraction coefficient ratio plots (appendix c) show that increasing the initial y-dimension causes less enthalpy extraction coefficient ratio increment than increasing the initial x-dimension. A gas flow with large clots is preferable to a gas flow with small clots and it is better to increase the initial x-dimension of the clot than the initial y-dimension. The Lorentz-force is higher for high temperature clots wich means that increasing the initial clot temperature from 3500 to 4100 K causes more clot expansion in y-direction. Still the high temperature clots appear to have a longer lifetime.

The load-factor is decreasing along the channel due to increase of clot velocity. Load-factor decrement means more internal dissipation increment than electrical power output increment:

$$k=\frac{E}{uB}=\frac{1}{1+\frac{P_{diss}}{P_{el}}} \qquad (6)$$

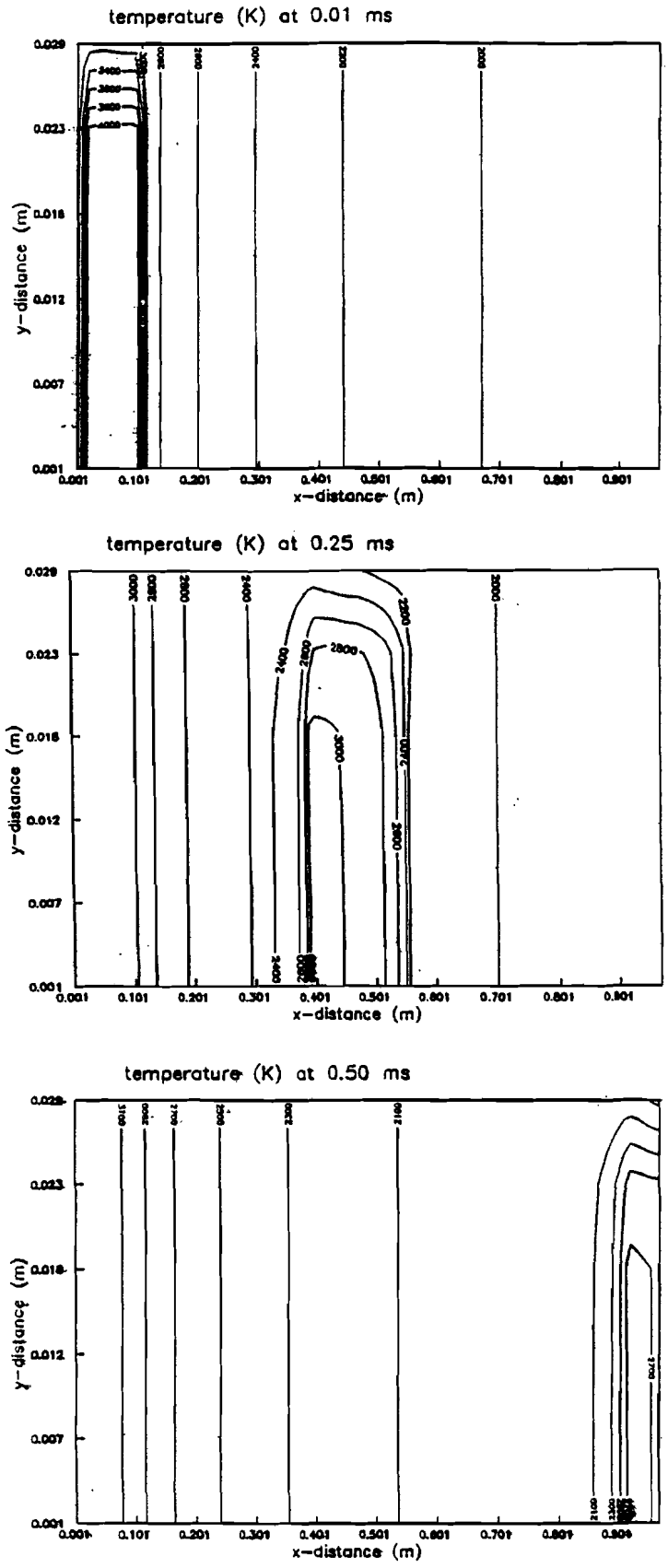

Figure 4.8 The x- and y- clot size at three successive time instants. The initial clot temperature is 4100 K and the initial x- and y-size are 10*5 cm.

5. THE MEASUREMENTS WITH THE EINDHOVEN ST-MHD FACILITY

The experiments have been carried out in the Eindhoven shock-tube facility [10]. The shock tube test gas consists of a mixture of CO and O_2. Due to the shock compression the test gas is heated above the ignition temperature for the combustion which provides for a high enough stagnation temperature to be of interest for the MHD experiments.

The configuration has been described before in chapter 3. The channel diverges in two directions from 58.4*58.4 mm^2 to 120.1*120.1 mm^2 at the channel exit over a length of 875 mm. The first electrode pair is situated at 75 mm downstream of the throat. There are 81 electrode pairs with an axial length of 1 mm. The segmentation length is 10 mm. The magnetic field is constant over the channel length and has a maximum of 2.5 T. The standard load is 5 ohm.

Hot plasma nonuniformities are formed by means of a discharge puls obtained from a capacitor of 1 μF charged to 6000 V at the 2^{nd} or 32^{nd} electrode pair.

Three aspects of the nonuniformities are considered more systematically as a function of the channel position: the clot current, the clot motion and clot dimension. The experiments with clot creation at electrode pair no. 32 and with magnetic induction of 1.5 T and 2.5 T are analysed.

5.1 RESULTS OF THE MEASUREMENTS

The current plots are presented in figure 5.1 and 5.2. Differences from run to run are often caused by different time instants of the discharge with respect to the current rise in the uniform plasma. It can be expected that the heating of the plasma by the discharge puls isn't reproducible. The dissipated energy density in the gas may be different due to different wall leakage and different arc dimensions.

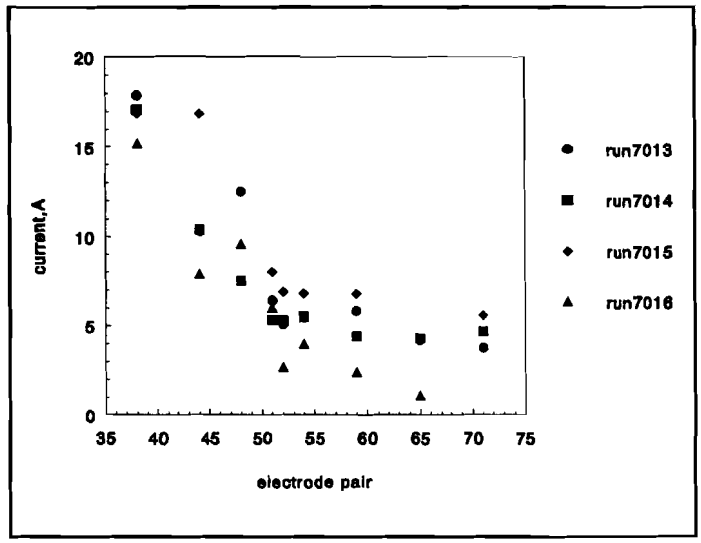

Figure 5.1 The maximum clot current for B = 1.5 T.

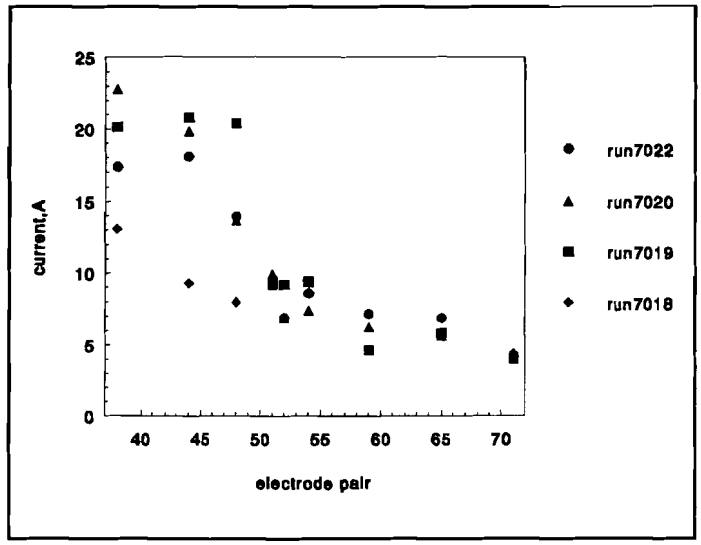

Figure 5.2 The maximum clot current for B = 2.5 T.

The motion of the clots is presented in figure 5.3 and 5.4. The scatter can mainly be attributed to the arbitrary way of determining the instant of passage from the voltage signals. The velocities of the clots are found to be equal to the gas velocity as determined from the open circuit voltages within the experimental error which is between 10 and 20 percent.

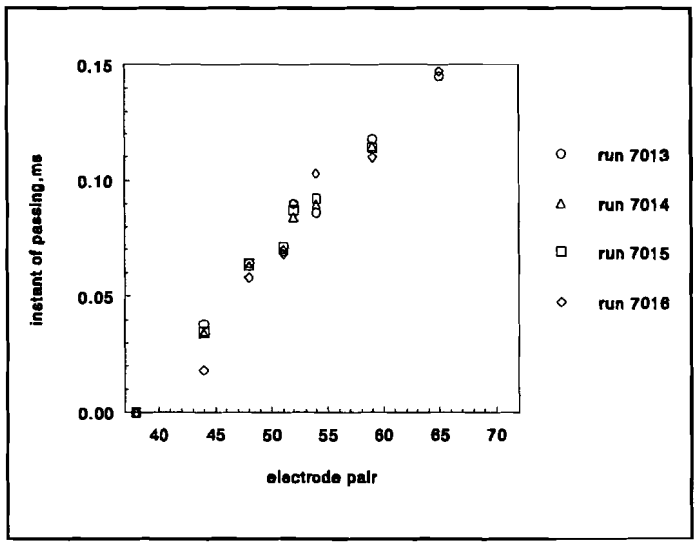

Figure 5.3 The passing instant of the clot maximum for B = 1.5 T.

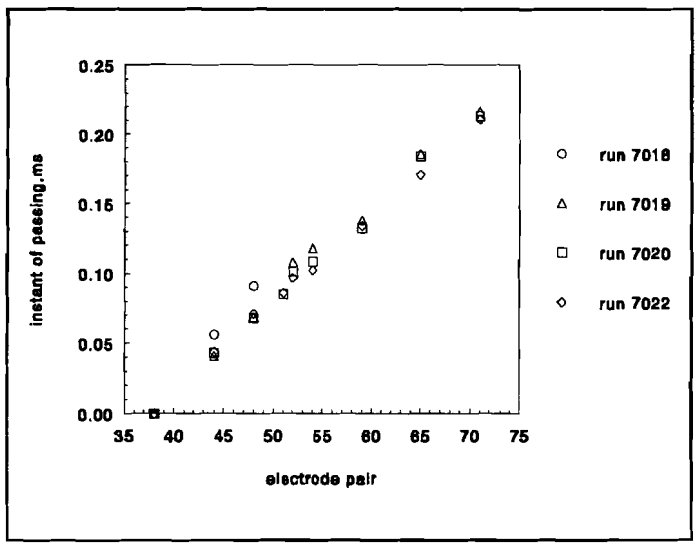

Figure 5.4 The passing instant of the clot maximum for B = 2.5 T.

The change of the clot geometry is presented in figure 5.5 and 5.6. The axial dimension of the clot is found from the time which they pass along the electrode pairs in combination with the velocities.

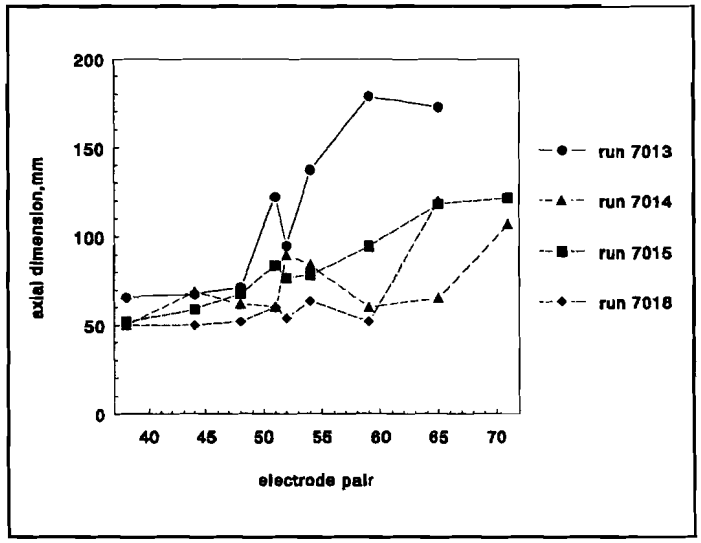

Figure 5.5 The axial clot dimension for B=1.5 T.

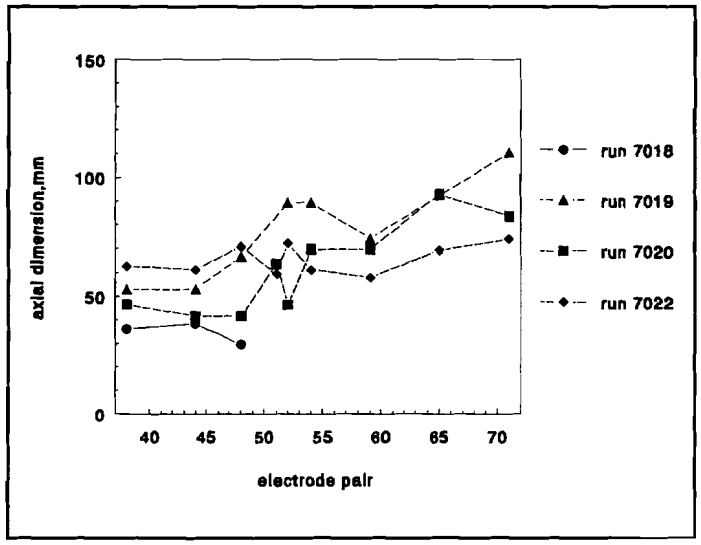

figure 5.6 The axial clot dimension for B=2.5 T.

The general trend of decreasing velocities with increasing magnetic induction can be observed from figure 5.3 and 5.4. Figure 5.1 and 5.2 show for the clot current two regions with different slopes; after the discharge location a fast decay of clot current can be observed, followed by a more smooth decay. Figure 5.5 and 5.6 show small increase of axial clot size just after creation and strong expansion in the second part of the channel.

Just after creation the clot is a high temperature, high pressure and well conducting area. The clot temperature is decreasing due to expansion in z-direction, the electric field direction, which explains the negative current gradient along the channel axis. Electron-ion recombination, thermal conduction and diffusion also account for the fast decay of the clot current after the discharge. The clot size in x- and y-direction increases in the second part of the channel which causes further clot temperature decrement.

In all considered cases the dissipation in the clots isn't large enough to keep the clot current at a constant level and prevent the clot decay. This indication is supported by the pressure measurements; no pressure fluctuations associated with the passage of the clot have been observed. The difference between the experiments with $B = 1.5$ T and 2.5 T is hardly significant. This indicates that the local magnetic interaction has to be increased considerably. To explain the fast clot decay electrode voltage drop, turbulence, diffusion, thermal conduction, viscosity, ion-electron recombination and the influence of the non-steady state gas flow have to be considered.

6. COMPARISON BETWEEN MEASUREMENTS AND SIMULATIONS

TUNOTANK

- The program considers uniform conditions in y- and z-direction, the clot is filling the channel cross-section completely.
- The clot is positioned in the quasi-steady state area of the flow train.
- The clot is moving through the whole channel.
- The channel divergence is double-sided.
- The clot is an high pressure and high temperature area.
- No thermal conduction,viscosity, turbulence and diffusion are considered.
- Ideal gas approximation and impermeable clots are considered.
- The generator is loaded with a constant load resistor.

FQ2SR

- The program considers uniform conditions in z-direction.
- The inlet conditions of the channel are steady state.
- The generator is loaded by a constant electric field.
- The clot is moving through the whole channel.
- The channel divergence is one-sided.
- The clot is a low mass density and high temperature area.
- No thermal conduction,viscosity, turbulence and diffusion are considered.
- Ideal gas approximation and impermeable clots are considered.

MEASUREMENTS

- The clot is positioned in a non-steady state area.
- The generator is loaded by a constant load resistor.
- The channel divergence is double-sided.
- The clot is a high pressure and high temperature area.
- Electrode boundary layers, thermal conduction, ion-electron recombination, diffusion, turbulence and viscosity have to be taken into account for the clot decay.
- The ideal gas approximation isn't valid and the clots are permeable.

7. CONCLUSIONS

Measurements show that clots can be created by means of a discharge. A decay of clot temperature along the channel is observed. Calculations consider no thermal conduction and diffusion and the clot temperature decreases along the channel due to clot expansion. The clot temperature decrement is high at the beginning of the channel and lower at the end of the channel. The clot height is equal to the channel height. For the 1-Dt calculations the clot width is equal to the channel width. The clot decelerates due to magnetic interaction and disturbes the gas flow. The result is a pressure gradient between clot and gas in channel width direction which causes clot width increment. The 2-Dt calculations show more clot expansion in channel width direction when the initial clot temperature increases from 3500 to 4100 K.

The clot creation mechanism for the measurements and the 1-Dt code provides for initial clots as high pressure and high temperature areas. The 1-Dt calculations show strong clot expansion just after creation. Thermal conduction, ion-electron recombination, turbulence and diffusion influences the clot expansion for the measurements. The 2-Dt code defines initial clots as low density and high temperate areas and no pressure gradient is present between the initial clot and the gas flow. The pressure gradient between clot and gas increases if internal dissipation takes place.

A second effect of the internal dissipation is less decay of clot temperature along the channel axis. High magnetic induction (5T) for the 1-Dt calculations causes high magnetic interaction and high internal dissipation which provides for a stable clot temperature. Measurements and calculations show that the internal dissipation for the condition of 2.5 T is too low to provide for a stable clot temperature. 1-Dt calculations for the condition of high boundary layer resistance support the indication that in case of the measurements the dissipation mainly takes place in the cold electrode boundary layers.

The initial clot length is increased from 5 to 15 cm for the 1-Dt calculations. For the 2D-t calculations the initial clot length is increased from 2.5 to 10 cm and the initial clot width from 2.5 to 5 cm. The calculations show that increasing the initial clot size extends the clot life time. A gas flow with large clots is preferable to a gas flow with small clots. It is better to increase the initial clot length than the initial clot width because of stronger clot deformation for large clot width due to gas flow disturbance.

The 1-Dt and 2-Dt calculations show a decreasing load factor along the channel, apparently the internal dissipation increases faster than the electrical power output.

It can be shown from the 2-Dt calculations that increasing the initial clot temperature from 3500 to 4100 K extends the clot lifetime. A clot with high temperature and long lifetime results in a high electrical power and energy output.

8. REFERENCES

[1] Veefkind, A. and W.F.H. Merck
THERMODYNAMISCH PERSPECTIEF MHD.
Energie Technologie, vol. 3, (1993), No. 5, p. 16-20.

[2] Sutton, G.W. and A. Sherman
ENGINEERING MAGNETOHYDRODYNAMICS
New York: Mc Graw - Hill book Comp., 1965.

[3] Ivanov, V.A. et al.
NUMERICAL SIMULATION OF EUT STF-MHD FLOW AND COAL PARTICLES IGNITION.
Internal report, Moscow: Institute for High Temperatures, 1992.
Academy of Sciences.

[4] Rietjens, L.T.Th.
ELEKTRISCHE ENERGIE.
Publ. 1988. Eindhoven: Eindhoven University of Technology.
Lecture notes nr. 5021.

[5] Veefkind, A. and W.F.H. Merck.
KOLEN EN ELECTRICITEIT.
Publ. 1990. Eindhoven: Eindhoven University of Technology.

[6] Bityurin, V.A. and A.P. Likhachev.
HIGH EFFICIENT MHD GENERATOR WITH SPACE AND TIME DEPENDENT CURRENT CARRYING NON-UNIFORMITIES.
Proc. 10th Int. Conf. on MHD Electr. Power Generation, Tiruchirappali India, 4-8 dec. 1989, vol. 2, p. 191-197.

[7] Bityurin, V.A. and A.P. Likhachev.
ON A PROBLEM OF EFFICIENCY OF THE MHD GENERATOR WITH SPACE- AND TIME DEPENDENT CURRENT CARRYING NONUNIFORMITIES.
Proc. 11th Int. Conf. on MHD Electr. Power Generation, Beijing China, oct. 1992, vol. 2, p. 666-674.

[8] Thijssen, G.H.C.M.
GASDYNAMICAL ASPECTS OF A NONUNIFORM CONDUCTING MHD CHANNEL FLOW.
Internal report. Publ. 1990. Eindhoven: Eindhoven University of Technology.

[9] Celinsky, Z.N. and F.W. Fischer.
TWO-DIMENSIONAL ANALYSIS OF MHD GENERATORS WITH SEGMENTED ELECTRODES.
Internal report. Publ. 1965. München: Institut für Plasmaphysic.

[10] Veefkind, A. et al.
SHOCK-TUBE EXPERIMENTS ON NON-UNIFORMITIES IN COMBUSTION MHD GENERATORS.
Proc. 31th. Int. SEAM Conf. on Engineering aspects of MHD, Montana U.S., 1993.

[11] Bityurin, V.A. et al.
MHD ELECTRICAL POWER GENERATION WITH PLASMA NONUNIFORMITIES - GAS INTERACTION.
Int. Spec. Meeting on Math. Modelling of MHD Power Stations, Eindhoven University of Technology, The Netherlands, 28-29 april 1986, p. 24-29.

[12] Vossers, G.
FYSISCHE TRANSPORTVERSCHIJNSELEN VR. W.
Publ. 1986. Eindhoven: Eindhoven University of Technology.
Lect. notes nr. 3438.

[13] Hirsch, C.
NUMERICAL COMPUTATION OF INTERNAL AND EXTERNAL FLOWS.
Part 1: Fundamentals of Numerical Discretization.
England: John Wiley & Sons, 1988.

[14] Hirsch, C.
NUMERICAL COMPUTATION OF INTERNAL AND EXTERNAL FLOWS.
Part 2: Computational Methods for Inviscid and Viscous Flows.
England: John Wiley & Sons, 1988.

APPENDIX A. THE HEAT CAPACITY FOR CO_2.

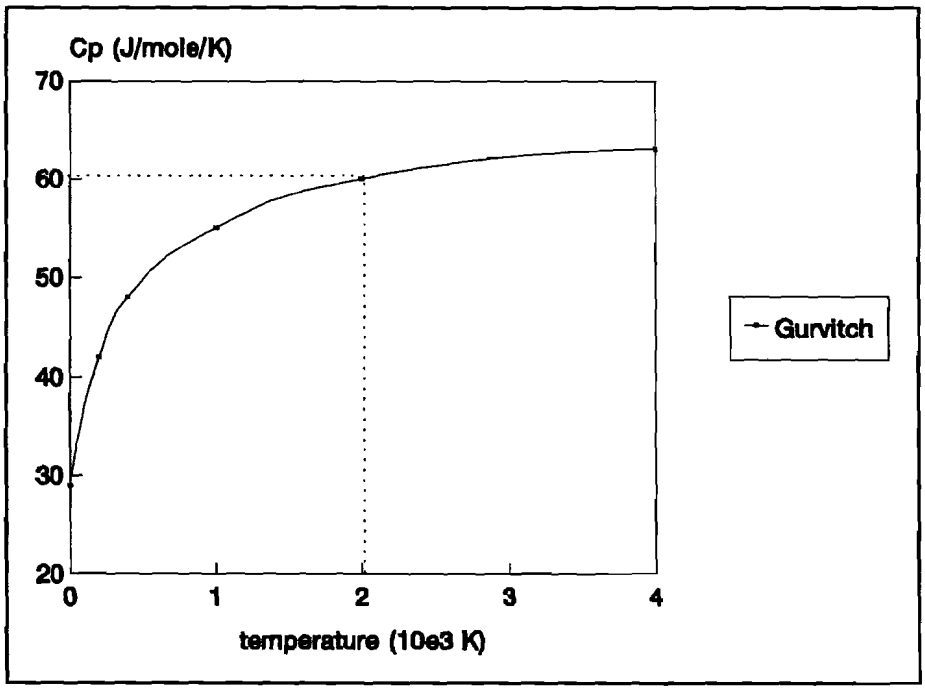

Figure A1. The C_p-value for CO_2 vs. temperature.

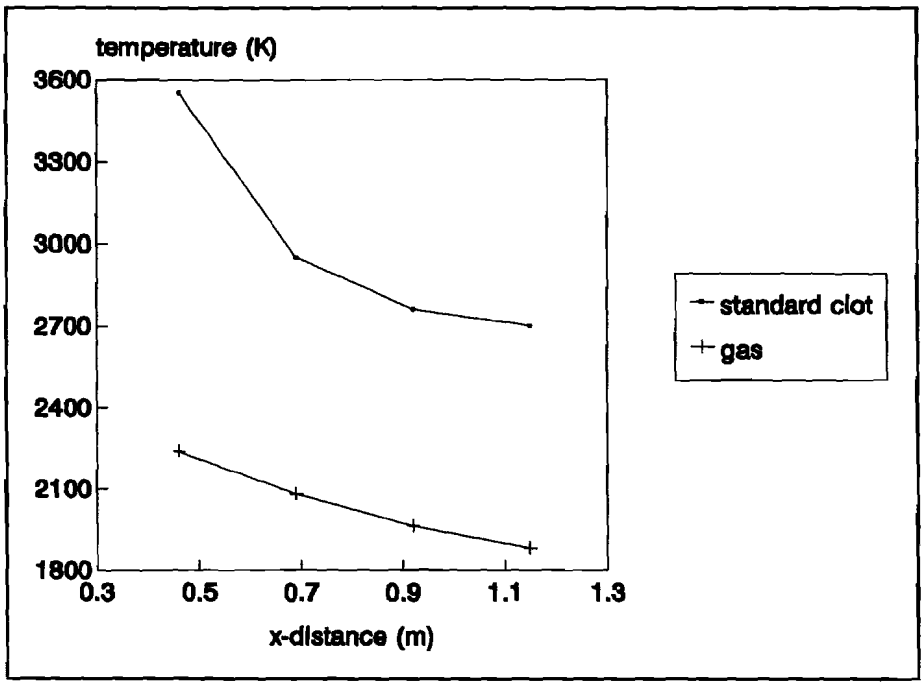

Figure B1. The clot and gas temperature.

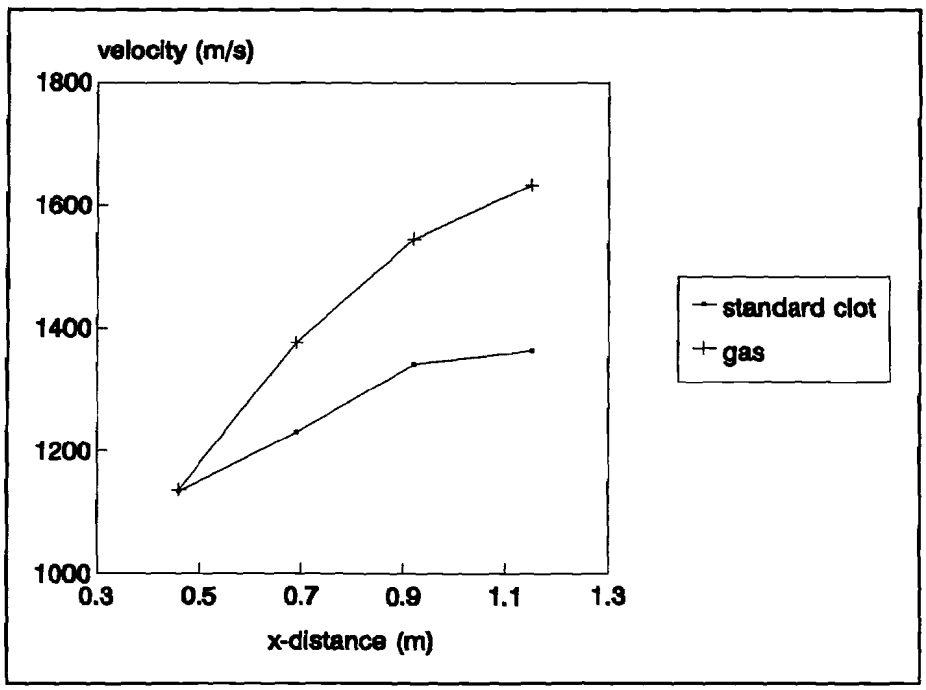

Figure B2. The clot and gas velocity.

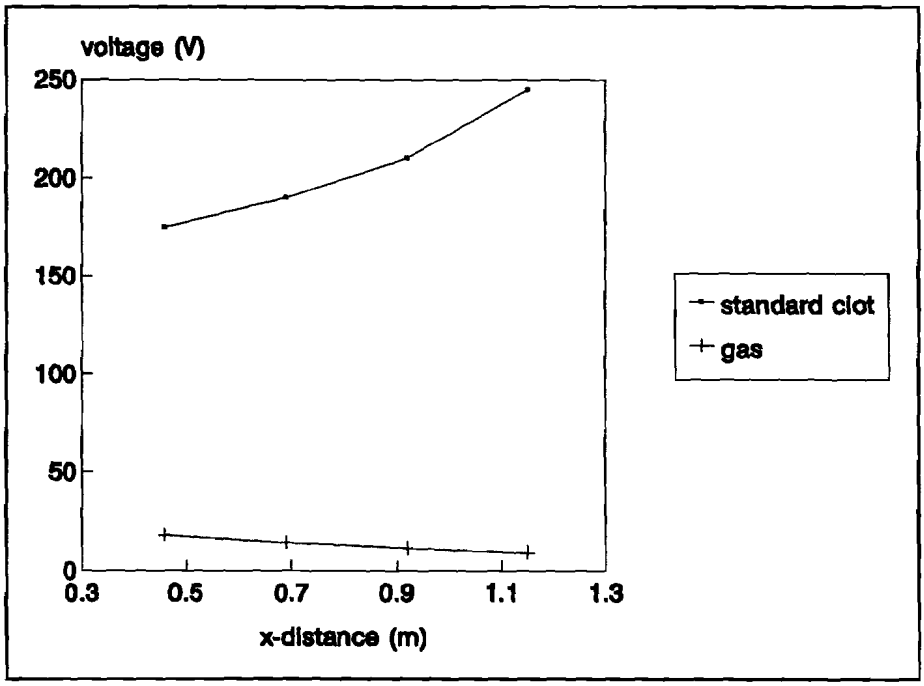

Figure B3. The clot and gas electrode voltage.

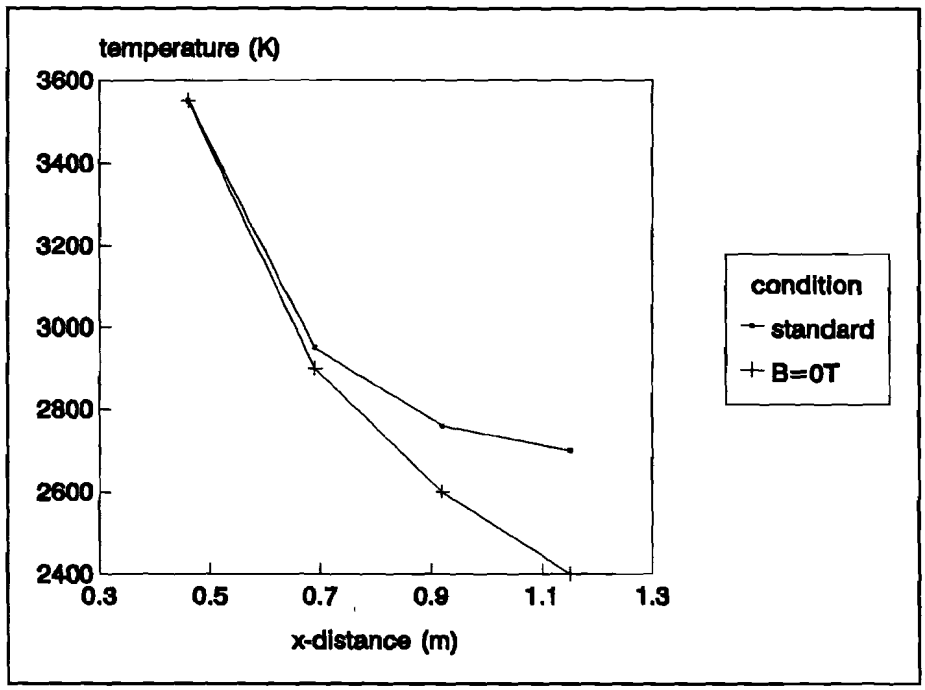

Figure B4. The clot temperature with and without magnetic interaction.

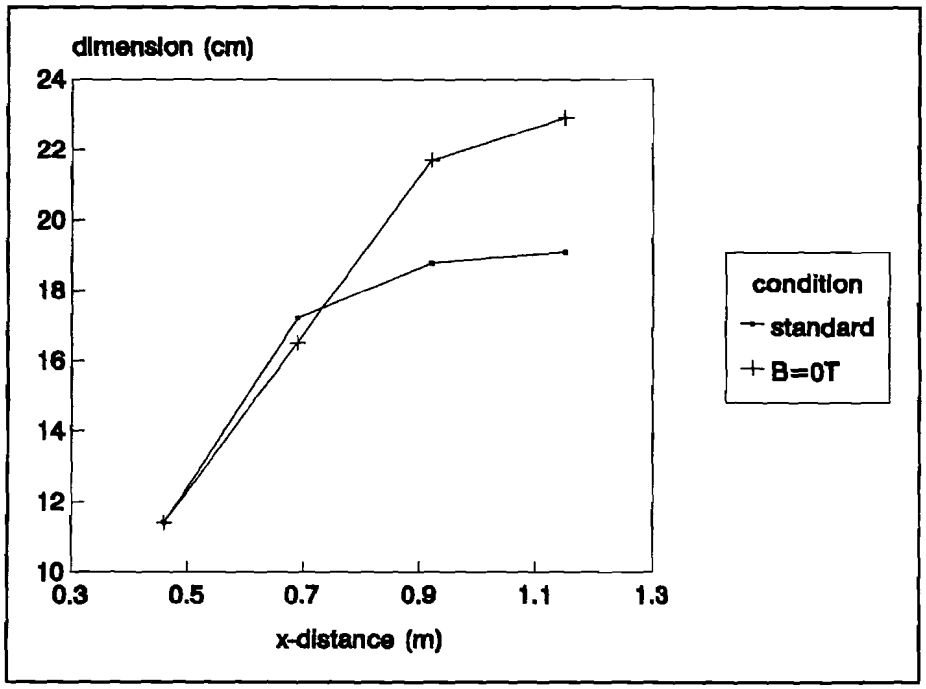

Figure B5. The axial clot size with and without magnetic interaction.

APPENDIX C. RESULTS OF THE FQ2SR SIMULATIONS.

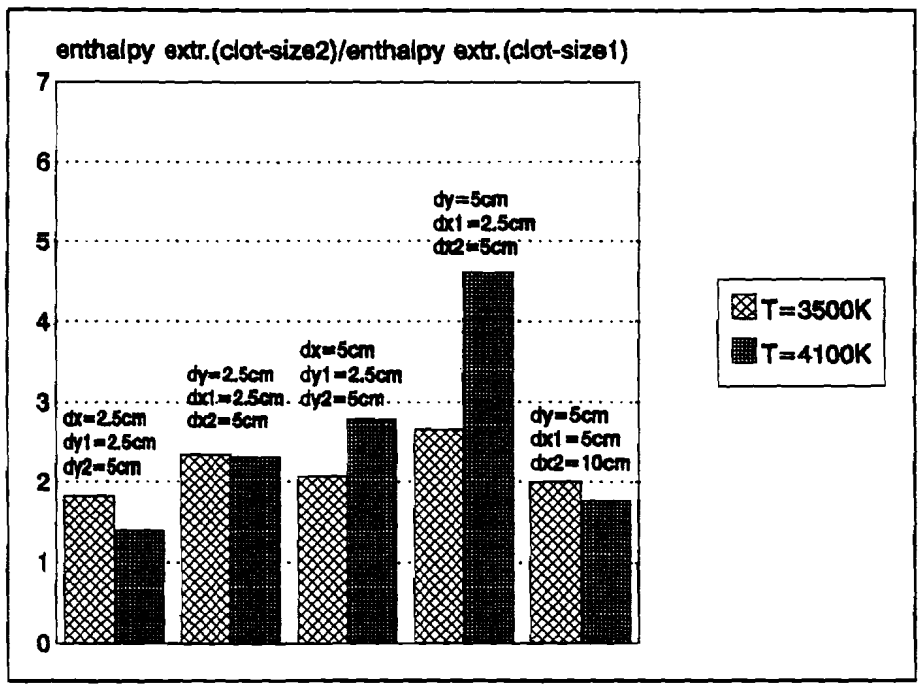

Figure C1. The enthalpy extraction increment ratio when the clot size increases.

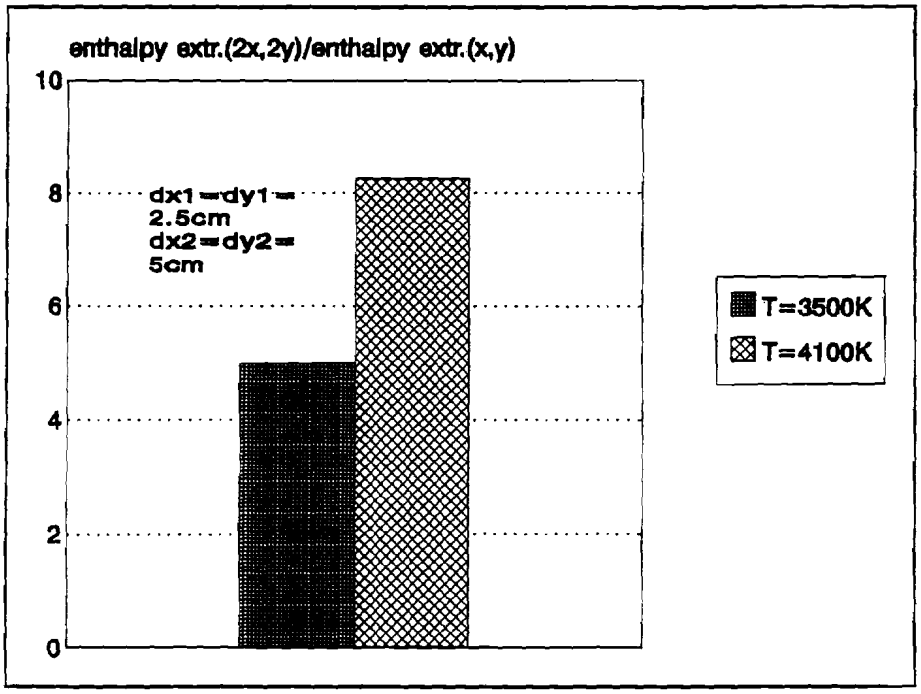

Figure C2. The enthalpy extraction coefficient ratio when the initial clot surface increases four times.

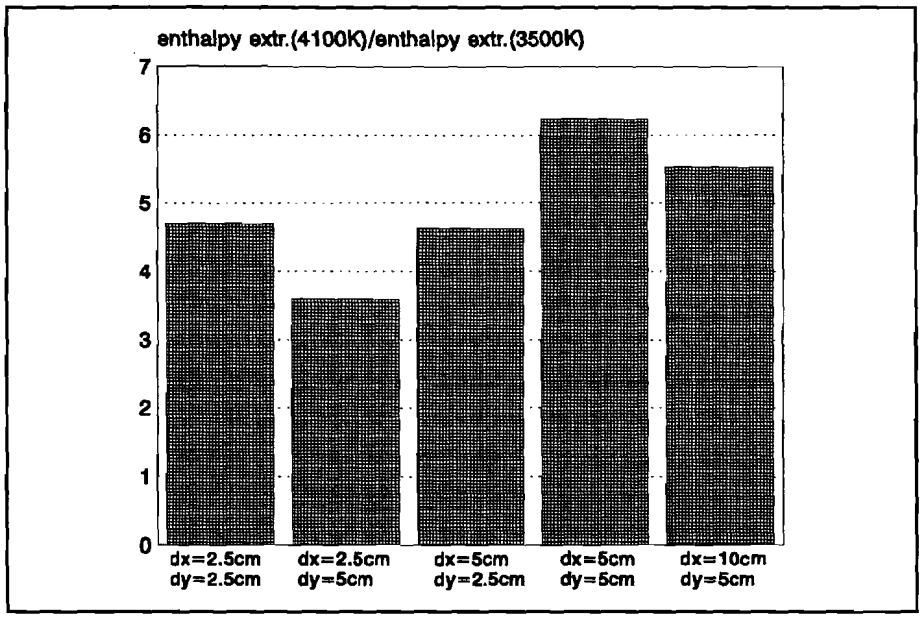

Figure C3. The enthalpy extraction increment ratio when the initial clot temperature increases.

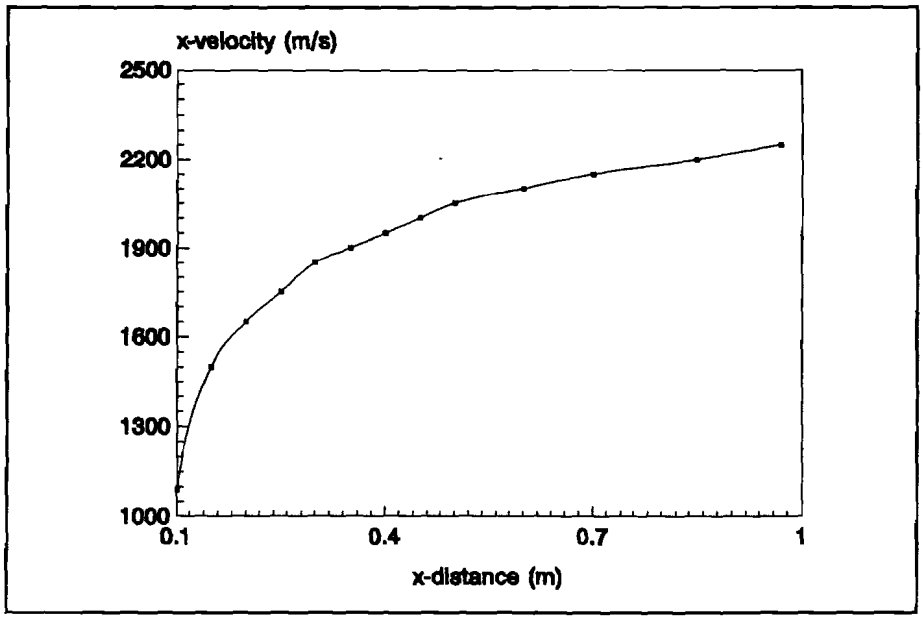

Figure C4. The gas velocity.